AGU100 ADVANCING EARTH AND SPACE SCIENCE

Geochemistry, Geophysics, Geosystems

RESEARCH ARTICLE
10.1029/2018GC007766

Gravitational Potential Energy per Unit Area as a Constraint on Archean Sea Level

Peter Molnar[1]

[1]Department of Geological Sciences and Cooperative Institute for Research in Environmental Sciences, University of Colorado Boulder, Boulder, CO, USA

Key Points:
- Equating gravitational potential energy beneath spreading centers and continents constrains chemical density anomalies
- Rare emergent early Archean continents constrain heat loss to approximately three times that today
- Emergence of continents at ~2.5 Ga is consistent with heat loss of twice that today

Correspondence to:
P. Molnar,
molnar@colorado.edu

Citation:
Molnar, P. (2018). Gravitational potential energy per unit area as a constraint on Archean sea level. *Geochemistry, Geophysics, Geosystems*, *19*, 4063–4095. https://doi.org/10.1029/2018GC007766

Received 15 JUN 2018
Accepted 6 OCT 2018
Accepted article online 13 OCT 2018
Published online 30 OCT 2018

Abstract To constrain the density structure of Archean lithosphere, I assume that gravitational potential energy (GPE) per unit area at Archean spreading centers equals that for continents whose surfaces lay near sea level. The present-day balance of GPE limits average density deficits in Archean mantle lithosphere due to depletion of iron during its formation to ~30–45 kg/m^3. For an Archean volume of seawater equal to or greater than that today and heat loss approximately three times that today (e.g., at ~3.5 Ga), plausible Archean structures, constrained by GPE balance, favor submerged spreading centers and continents. Emergent Archean continents would be allowed by a combination of the following (a) heat loss only twice that today, (b) less than approximately half of the present-day volume of thick crust, either continental or oceanic plateaus, and (c) deep Archean spreading centers ($\gtrsim$2 km below continents), which would require a thickness of Archean oceanic crust $\lesssim$25 km. If the volume of Archean seawater were 50% greater than that today, emergent spreading centers could have existed only as isolated unusual features, and emergent continents would require both limited extent of thick crust and spreading centers deeper that ~2 km. The observed widespread development of continental margins and carbonate platforms at ~2.7–2.5 Ga is consistent with heat loss roughly twice that today, a volume of seawater comparable with that today, and either (a) a volume of continental crust comparable to that at present and oceanic crust $\lesssim$30 km thick or (b) thicker oceanic crust, possibly 40–50 km, but with a volume of continental crust less than approximately half that today. Calculated temperatures at the Archean Moho are ~700–900 °C. These calculations do not rule out a hot early Archean ocean (~50–80 °C) and do not favor an early Archean emergence of life on land above sea level.

1. Introduction

The date when land surface, whether basaltic ocean floor or continental crust, emerged above sea level bears on questions as diverse as the thermal history of the Earth's interior (e.g., Jaupart, et al., 2015; Korenaga, 2008a, 2008b; Labrosse & Jaupart, 2007), the temperature of seawater in early Archean time (e.g., Jaffrés et al., 2007; Kasting et al., 2006), and the origin of life (e.g., Mulkidjanian, 2009; Sutherland, 2016). I seek bounds on that date using simple arguments that relate cooling of a thermal boundary layer of the convecting mantle (including plates of rigid lithosphere, when plate tectonics operates), the potential temperature of the upper mantle, the thickness of Archean oceanic crust, the lateral extent and thickness of Archean continental crust, and plausible amounts of post-Archean erosion of that crust, with allowance for a greater volume of seawater than that today. Because of the large uncertainties in requisite parameters, definitive statements must follow from numerous assumptions of both processes and parameters that quantify them (Table 1).

As have others in similar studies, I assume local isostatic equilibrium. Following England and Bickle (1984) for Archean time and others for the present (e.g., Doin et al., 1996; England & Houseman, 1989; Haxby & Turcotte, 1978; Turcotte & McAdoo, 1979), I also assume that the gravitational potential energy (GPE) per unit area for spreading centers equals that for low continents, whose surfaces are at or near sea level. Imposing this balance tightens constraints on the deficit in density of Archean mantle lithosphere associated with depletion of iron during its formation, as Jordan, (1975, 1978, 1988) proposed.

2. Geologic Background

Despite the small amount of Archean crust that crops out today (e.g, Hurley & Rand, 1969), many imagine that most of the Earth's crust had formed by the end of the Archean Eon or by early Proterozoic time (~2 Ga;

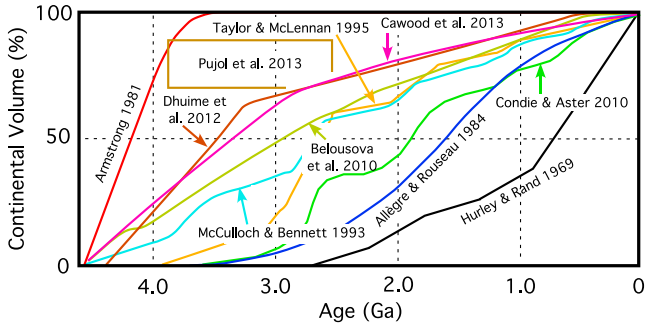

Figure 1. Inferences of growth of continental crust expressed as a fraction of the present-day volume.

e.g., Abbott & Hoffman, 1984; Armstrong, 1968, 1981; Belousova et al., 2010; Bowring & Housh, 1995; Campbell, 2003; Cawood et al., 2013; DePaolo, 1983; Dhuime et al., 2012, 2015; Hofmann et al., 1986; Kröner, 1985; Pujol et al., 2013; Reymer & Schubert, 1984; Taylor & McLennan, 1995; Wise, 1974; Figure 1). From differences in radiogenic isotopes, like ^{143}Nd, between crust and mantle, others (e.g., Allègre & Rousseau, 1984; Collerson & Kamber, 1999; Goldstein et al., 1984; Hawkesworth & Kemp, 2006; McCulloch & Bennett, 1993, 1994; Nelson & DePaolo, 1985) have envisioned steady growth of crust with more post-2.5-Ga than pre-2.5-Ga growth (Figure 1). From clustered populations of U-Pb ages of zircons, some have inferred pulsed additions of crust (e.g., Arndt & Davaille, 2013; Belousova et al., 2010; Condie & Aster, 2010; Taylor & McLennan, 1995; Figure 1), and a few have challenged various inferences by questioning the certainty with which initial values of isotopes can be assigned (e.g., Arndt & Goldstein, 1987; Sylvester et al., 1997). Although one of these studies may correctly describe the history of continental growth, few seem to agree on, l et alone know, which that study is.

Jordan, (1975, 1978, 1988) suggested that in the formation of Archean crust the extraction of iron during melting reduced the density of the uppermost mantle sufficiently to sustain surface heights above sea level. Abundant evidence now calls for mantle lithosphere beneath Archean terrain less dense than asthenosphere at the same temperature and pressure (e.g., Arndt et al., 2009; Doin et al., 1996; Poudjom Djomani et al., 2001; Schutt & Lesher, 2010; Shirey et al., 2002; Turcotte & McAdoo, 1979). Moreover, since Brune and Dorman (1963)

Table 1
List of Symbols Used

Name	Symbol (and value)
Depth to base of continental lithosphere	L (200–300 km)
Thickness of continental crust	h_{cc} (30–60 km)
Thickness of oceanic crust	h_{oc} (7 km, today)
Height of surface of low continents	δh_c (0–300 m, today)
Height of water above low continents	h_{lc}
Depth of spreading center	h_{mor} (2,600 ± 200 m, today)
Density of see water	ρ_w (1.0×10^3 kg/m^3)
Density of oceanic crust	ρ_{oc} ($2.9–3.1 \times 10^3$ kg/m^3)
Density of continental crust	ρ_{cc} ($2.7–2.9 \times 10^3$ kg/m^3)
Density of the asthenosphere	ρ_a ($3.2–3.3 \times 10^3$ kg/m^3)
Density deficit of Archean mantle lithosphere	$\delta\rho_c(z)$
Mean density deficit of Archean mantle lithosphere	$\overline{\delta\rho_c}$
Temperature of the asthenosphere	T_a (1350–1650 °C)
Temperature at Moho beneath continents	T_{Moho} (350–5500 °C)
Age of oceanic lithosphere	t(<200 Myr)
Maximum age of oceanic lithosphere	t_m (~200 Myr, today)
Coefficient of thermal conductivity	k (3 W·m^{-1}·K^{-1})
Coefficient of thermal diffusivity	κ (10^{-6} m^2/s)
Coefficient of thermal expansion	α ($3–4 \times 10^{-5}$ °C^{-1})
Heat loss from the Earth	Q
Present-day heat loss from the Earth	Q_0 (42 ± 2 TW)
Volume of water in today's ocean and ice	V_w (1.36×10^9 km^3)
Volume of the ocean basin	V_0
Area of the ocean basin	A_0
Area of the Earth	A_E (5.10×10^8 km^2)
Coefficient, a, relating depth to age of ocean floor	$\frac{2\rho_a \alpha T_a \sqrt{\kappa}}{\sqrt{\pi}(\rho_a - \rho_w)}$ (320 m/Myr$^{\frac{1}{2}}$)

Table 2
Archean Crustal Thicknesses

Region and reference	Thickness
Southern part (Tseng & Chen, 2006)	36 ± 2 km
Singhbhum Craton, NE India (Singh et al., 2017)	>50 km
Eastern Dharwar Craton (Borah et al., 2014)	34–38 km
Eastern Dharwar Craton (Gupta et al., 2003)	34–39 km
Eastern Dharwar Craton (Saikia et al., 2017)	35 ± 1 km
Eastern Dharwar Craton (Singh et al., 2017)	<35 km
Western Dharwar Craton (Borah et al., 2014)	~50 km
Western Dharwar Craton (Das et al., 2015)	~40 km to >50 km
Western Dharwar Craton (Gupta et al., 2003)	42–51 km
Western Dharwar Craton (Saikia et al., 2017)	39 ± 1 km
Western Dharwar Craton (Singh et al., 2017)	>55 km
Slave Craton (Bank et al., 2000)	37 to 40 km
Rae Craton (Thompson et al., 2010)	34 to 42 km
Rae Craton (Snyder et al., 2015)	35 to 42 km
Hearn Craton (Thompson et al., 2010)	~38 km
Rae, Hearn,and Superior Cratons (Gilligan et al., 2016)	34–42 km
Superior Craton (Darbyshire et al., 2007)	32 to 48 km
Western Superior Province (Musacchio et al., 2004)	32 to 45 km
Western Superior Province (Angus et al., 2009)	38 to 47 km
Zimbabwe Craton (Kgaswane et al., 2009)	36.2 ±1.2 km
Zimbabwe Craton, Tokwe block (Youssof et al., 2013)	35–38 km
Zimbabwe Craton, Tati block (Youssof et al., 2013)	47–51 km
Kaapvaal Craton (de Wit & Tinker, 2004)	36–41 km
Kaapvaal Craton (James et al., 2003)	35 km
Kaapvaal Craton (Kachingwe et al., 2015)	38–39 ± 3 km
Kaapvaal Craton (Kgaswane et al., 2009)	37–39 km
Kaapvaal Craton (Nair et al., 2006)	38 km
Kaapvaal Craton (Niu & James, 2002)	35.4 ± 0.2 km
Kaapvaal Craton (Youssof et al., 2013)	35–40 km
Kaapvaal and Zimbabwe Cratons (Delph & Porter, 2014)	~34 km
Kaapvaal and Zimbabwe Cratons (Nguuri et al., 2001)	35–40 km
Pilbara Carton (Reading & Kennett, 2003)	30 ± 2 km
Pilbara Carton (Drummond, 2003)	~30 km
Yilgarn Carton (Reading & Kennett, 2003)	40 ± 2 km

demonstration of a thick high-speed layer beneath the Canadian Shield, seismological studies using both surface waves (e.g., Debayle & Ricard, 2012; Jordan, 1975; Shapiro & Ritzwoller, 2002; Toksöz et al., 1967) and multiply reflected *S* waves (e.g., Grand & Helmberger, 1984) have repeatedly confirmed thick Archean lithosphere. Improved estimates of heat-producing elements and measurements of heat flux through the Earth's crust have demonstrated low heat flux transferred to the base of the continental lithosphere, which in turn requires thicknesses of ~200–250 km for the conducting lid over the convecting asthenosphere (e.g., Jaupart & Mareschal, 1999, 2011; Jaupart et al., 1998, 2014; Michaut et al., 2007).

More remarkable is the demonstration that such thicknesses were established in Archean time: by Archean dates of diamonds (e.g., Boyd & Gurney, 1986; Boyd et al., 1985; Richardson et al., 1984; 2001), by Re-Os model ages (e.g., Carlson et al., 1999, 2005; Irvine et al., 2001; Pearson, Carlson, et al., 1995, Pearson, Snyder, et al., 1995; Shirey et al., 2001; Westerlund et al., 2006), and by other geochemical indicators (e.g., Bedini et al., 2004; Bickle, 1978; Canil et al., 2003; Carlson et al., 2000; Schoene et al., 2009). By contrast, the lower crust in many regions seems to have been quite hot, presumably because of greater radiogenic heat production then than now.

Table 3
Suggested Thicknesses of Archean Oceanic Crust

Thickness	Reference
~10 km	Vlaar (2000)
<20 km	van Thienen et al. (2004)
20–25 km	Sleep and Windley (1982)
21 ± 2km	Galer and Metzger (1998)
25 km	Hynes (2001)
27 km	Abbott et al. (1994)
25–35 km	Herzberg et al. (2010)
30–45 km	Herzberg and Rudnick (2012)
42 km	Galer (1991)

Inferences of temperatures at pressures corresponding to depths of 30–35 km reach 700 °C, to perhaps 900 °C (e.g., Bickle, 1978; Davis et al., 2003; Grambling, 1981; Jaupart & Mareschal, 2015; Johnson et al., 2017; Michaut et al., 2009; Perkins & Newton, 1981; Rey & Coltice, 2008; Rey & Houseman, 2006; Singh, 2015), although Burke and Kidd (1978) argued for lower temperatures from the absence of melting of crust.

Thicknesses of present-day Archean crust vary from ~30 to ≳50 km (Table 2), but such differences seem to be isostatically compensated by differences in both mean densities of crust and density deficits in mantle lithosphere. The presence of xenoliths rich in garnet and of other dense minerals from Archean lower crust suggests that mean densities of Archean crust, at least in some regions, are greater than those of Proterozoic crust (e.g., Hacker et al., 2015; Mahan et al., 2012). Tang et al. (2016) reported a markedly mafic composition of early and middle Archean crust, a view similar to Rollinson's (2017). Moreover, granulite, with relatively high density, is common in Archean outcrops (e.g., Davis et al., 2003; Rudnick & Fountain, 1995; Taylor & McLennan, 1995).

Because half-lives of heat-producing radiogenic isotopes (U^{238}, Th^{232}, and K^{40}) are comparable to the age of the Earth, heat production in Archean time was greater than that today. Wasserburg et al. (1964) inferred that heat production at 4.5 and at 3 Ga would have been 4 and 2.2 times that today, respectively. McKenzie and Weiss (1975) approximated heat production as a single exponential with an *e*-folding time of 3,248 Myr, which calls for heat production 2.16, 2.52, 2.94, and 3.42 times that today at 2.5, 3.0, 3.5, and 4.0 Ga, respectively. These values differ little from those offered by Davies, (1979, 1980), Richter, (1984, 1985, 1988), and Schubert et al. (1980). Of course, heat loss, which includes primordial heat and the GPE loss associated with the formation of the core, needs not keep pace with heat production (e.g., Christensen, 1984, 1985; Davies, 1979, 1980; Jaupart, Labrosse, et al., 2015; McKenzie & Richter, 1981; McKenzie & Weiss, 1975; Richter, 1986). The Urey ratio, the ratio of heat produced in the mantle to that lost through the ocean floor and the base of continental crust, Q_0, is determined to be $Ur \approx 0.3$ ($0.12 \leq Ur \leq 0.49$; e.g., Jaupart, Labrosse, et al., 2015; Labrosse & Jaupart, 2007).

Efforts to estimate the evolution of heat loss over time rely on assumptions for when vigorous convection began. McKenzie and Weiss (1975) inferred heat loss would also have been decaying exponentially with time by early Archean time. Most estimates of Archean heat loss are $Q(3.5\ \text{Ga}) \approx 3Q_0$ and at $Q(2.5\ \text{Ga}) \approx 2Q_0$ (e.g., Christensen, 1984; Davies, 1979, 1980; McKenzie & Richter, 1981; McKenzie & Weiss, 1975; Richter, 1984, 1985; Schubert et al., 1980), though Christensen (1985) suggested that Archean heat loss might have been smaller, $\sim 2Q_o$ at 3.5 Ga, and Korenaga, (2006, 2007, 2008b) suggested that heat loss has changed little since Archean time.

Most associate the greater Archean heat generation with a hotter mantle than that today. Inferences of temperatures at which melting of the mantle gave rise to basalt that did not form at subduction zones (nor as komatiites) call for potential temperatures in Archean time that were ~150–250 °C warmer than those today, and therefore ~1500–1600 °C (e.g., Abbott et al., 1994; Bickle, 1986; Grove & Parman, 2004; Herzberg et al., 2010; Jaupart & Mareschal, 2011; Keller & Schoene, 2018; Lee & Chin, 2014; Nisbet et al., 1993), though Flament et al. (2008) and Ganne and Feng (2017) argued for a smaller difference. With an adiabatic gradient of ~0.4 °C/km, temperatures at 200 km would have been ~1600–1700 °C. Although heat production surely

decreased during Archean time, and heat loss presumably did as well, cooling of the mantle may have been slight, before steady cooling began at ~2.5 Ga (Herzberg et al., 2010).

A higher potential temperature means that upwelling mantle at spreading centers should begin to melt at greater depths, and more rock should melt than at mid-ocean ridges today. Thus, most assume that Archean oceanic crust was thicker than today's 7 km (e.g., White et al., 1992). Inferred thicknesses of Archean ocean crust range from ~10 to 45 km (Table 3). Some have drawn an analogy with conditions that produced the Ontong Java plateau (e.g., Fitton & Godard, 2004; Herzberg & Rudnick, 2012), where crust is ~30 km thick, and others with those at present-day hot spots (e.g., Putirka, 2005, 2008; Reimink et al., 2014). Kamber (2010), in fact, inferred that volcanic plateaus were far more extensive in Archean than present time. In estimating Archean sea level, I treat such regions of thick crust as continents, but clearly, the average density of that crust could have been different from what characterizes Archean crust today. Moreover, if normal Archean oceanic crust were as thick as 35 km or more, distinguishing it from oceanic plateaus adds an another uncertainty.

Regarding Archean sea level, many have argued that little continental crust stood above it (e.g., Arndt, 1999; Ernst et al., 2016; Flament et al., 2008; Lee et al., 2017; McCulloch & Bennett, 1994). Buick et al. (1995), however, reported an angular unconformity that they associated with subareal erosion and deposition, overlain by a tuffaceous sandstone that they correlated with nearby sedimentary rock containing zircons dated at 3.46–3.47 Ga. Thus, they inferred that crust below the unconformity was emergent at ~3.45 Ga. For the slightly younger Strelley Pool Chert, ~3.4 Ga, Lowe (1983) reported deposition in shallow water, but his emphasis on "the extreme paucity of detrital quartz, an inevitable product of the weathering and erosion of continental blocks" suggests that nearby emergent terrain was sparse. Early Archean deposition in South Africa seems to have been dominated by deep water sediment (e.g., Lowe, 1980). Trower and Lowe (2016) described the Mendon Formation in the Barberton Greenstone Belt in South Africa as deposited in a submarine environment between 3.5 and 3.26 Ga. Moreover, in part from the *paucity of shale*, Lowe (1980) stated that "there could not have been any large land areas of either low or high relief in or adjacent to these greenstone basins" in South Africa, Australia, or India between ~3.5 and ~3.1 Ga. Although sedimentary archives indicating early Archean subaerial deposition seem sparse, some conglomeratic deposits do suggest subareal erosion at that time (e.g., Lowe, 1999; Lowe & Byerly, 1999; Lowe & Fisher Worrell, 1999). In addition, the mineral nahcolite ($NaHCO_3$), which is associated with evaporation on land, has been found in 3.2- to 3.5-Ga rock from the Barberton region of South Africa (e.g., Lowe & Fisher Worrell, 1999; Lowe & Tice, 2004) and therefore also suggests exposure to the atmosphere. It follows that if early to middle Archean rock lay emergent above sea level, such occurrences were not widespread.

Evidence of emergent terrain seems to increase with rock deposited at ~3.3–3.2 Ga. Heubeck and Lowe (1994) reported that the 3.2- to 3.2-Ga Moodies Group for the Barberton region was deposited subaerially as alluvial conglomerate overlain by braided fluvial, tidal, and deltaic sandstones. Kamo and Davis (1994) differed from Heubeck and Lowe (1994) regarding provenance, but they, too, inferred fluvial and shallow coastal environments. Satkoski et al. (2016) used relatively high $^{87}Sr/^{86}Sr$ ratios, >0.701, in 3.26-Ga barite deposited in a marine environment to deduce that by this time continental crust was being weathered sufficiently to affect $^{87}Sr/^{86}Sr$ ratios.

Evidence of exposed late Archean terrain is relatively abundant. Bickle et al. (1975) inferred that between 2.8 and 2.5 Ga, a typical continental margin had formed in the Belingwe greenstone belt of Rhodesia. Beukes (1984) inferred the same: "deposition in a wide variety of sedimentary environments ranging from basinal to shallow epeiric sea, supratidal flat and fresh-water lake" for the Campbellrand Subgroup in South Africa, a result substantiated with further analysis (e.g., Beukes, 1987; Sumner & Beukes, 2004). Bradley (2008) synthesized data to suggest that passive margins adjacent to exposed continents have been around since 2.74 Ga, a view shared by Campbell and Davies (2017), though de Wit et al. (1992) argued for earlier margins, near 3.1 Ga. Eriksson et al. (2006), in fact, described fluvial sediment, which they associated with braided streams, from South Africa (the Dominion Group) at ~3.1–3.0 Ga. They argued that evidence of emergent continents earlier in Archean time can be found from other regions, including Australia and India.

In summary, exposure of middle Archean, ~3.5 Ga, continents seems to have been sparse, but not absent. By late Archean time, however, exposed continents seem to have been widespread, and continental margins like those today seem to have formed.

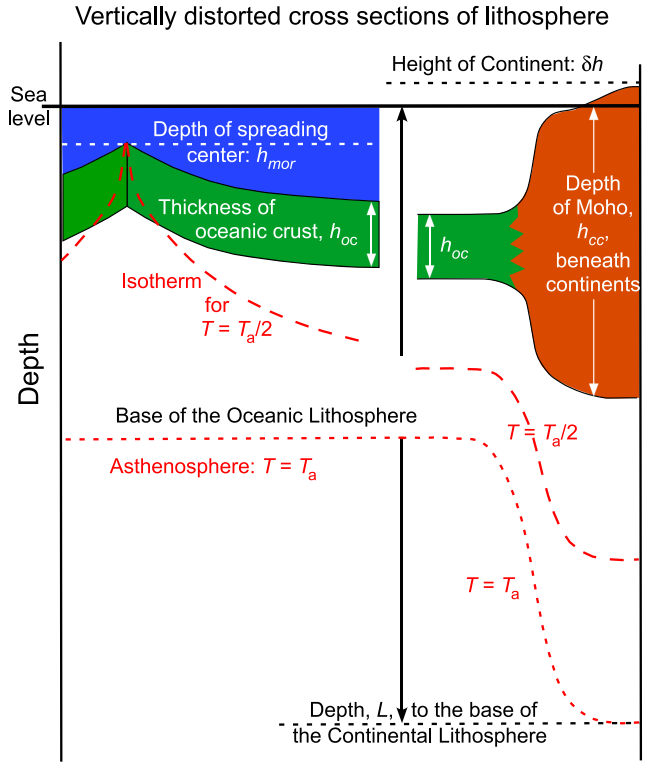

Figure 2. Distorted cross sections through oceanic lithosphere near spreading centers (left) and beneath old ocean floor and adjacent continents (right) defining various thicknesses and depths. Depths of the ocean, thickness of crust, and heights above sea level are exaggerated.

Not least controversial among Archean conditions is the volume of the seawater. Many assume the same as that today (e.g., Abe & Matsui, 1988; Allègre et al., 1983; Cogley & Henderson-Sellers, 1984; Matsui & Abe, 1986; McGovern & Schubert, 1989), but a constant volume requires a remarkably delicate balance (Fyfe, 1978). At the current rate that water is subducted into the mantle, if only 80% were released to the surface again, sea level would drop at 1 m/Myr, or 1 km in 1 Gyr (Jarrard, 2003). Korenaga (2008a) suggested that the Archean volume was twice that today and later revised his estimate to ~50 ± 25% greater (Korenaga, 2011).

3. Isostasy

Most considerations of Archean crustal and mantle structure begin with the assumption of isostatic equilibrium, and therefore, the column of mass per unit area to the depth of the base of the thickest lithosphere is the same:

$$\int_{\text{Surface}}^{L} \rho(z)\mathrm{d}z = \text{Constant}, \tag{1}$$

where L is the depth to the base of the continental lithosphere, ρ is density, and z is depth, positive downward (Figure 2).

Beneath a mid-ocean ridge today or beneath Archean spreading centers, the potential temperature is constant and equal to that in the asthenosphere. Thus, a column of mass per unit area above a depth L is given by the following:

$$\frac{\text{Mass}}{\text{Area}} = \rho_w h_{\text{mor}} + \rho_{\text{oc}} h_{\text{oc}} + \rho_a (L - h_{\text{mor}} - h_{\text{oc}}), \tag{2}$$

ρ_w is the density of water, h_{mor} is the depth of the spreading center below sea level, ρ_{oc} is the mean density of oceanic crust, h_{oc} is the thickness of oceanic crust, and ρ_a is the density of asthenosphere, assumed constant because the temperature gradient is, on average, adiabatic in the asthenosphere. Compression due to increasing pressure with depth can be ignored, because lateral differences in pressure are small compared with lithostatic pressure.

For continental lithosphere, the (uncompressed) density in the mantle decreases with depth because of increasing temperature in it. As the thermal time constant for conductive heating of lithosphere ~200–300 km thick is comparable to the half-lives of some major heat-producing radiogenic elements, the temperature structure of thick Precambrian lithosphere has never reached steady state but evolves continuously (e.g., Michaut & Jaupart, 2004; Michaut et al., 2007). Nevertheless, the simplest approximation is that temperature increases linearly with depth from the Moho to the base of the lithosphere, much more steeply than the adiabatic gradient. Let T_a (≈ 1350 °C = 1623 K today; e.g., McKenzie & Bickle, 1988; Sarafian et al., 2017) be the potential temperature of the asthenosphere and hence both the temperature at the base of the continental lithosphere and the essentially constant temperature in the mantle beneath spreading centers. With T_{Moho} the temperature at the continental Moho, at depth h_{cc} and $\Delta T_0 = T_a - T_{\text{Moho}}$, a linear increase in temperature with depth through the mantle lithosphere is given by the following:

$$\Delta T(z) = \Delta T_0 \frac{L - z}{L - h_{\text{cc}}}; h_{\text{cc}} \le z \le L. \tag{3}$$

Density in the mantle lithosphere beneath continents ($h_{\text{cc}} \le z \le L$) is as follows:

$$\rho(z) = \rho_a - \delta\rho_c(z) + \rho_a \alpha \Delta T(z) = \rho_a - \delta\rho_c(z) + \rho_a \alpha \Delta T_0 \frac{L - z}{L - h_{\text{cc}}}, \tag{4}$$

where $\delta\rho_c(z)$ is the density anomaly in the mantle due to the depletion of iron and α is the coefficient of thermal expansion. With ρ_{cc} the mean density of continental crust and δh_c the height of the continent above sea level, at $z = L$,

$$\frac{\text{Mass}}{\text{Area}} = \rho_{\text{cc}}(h_{\text{cc}} + \delta h_c) + (\rho_a - \overline{\delta\rho_c})(L - h_{\text{cc}}) + \frac{1}{2}\rho_a \alpha \Delta T_0 (L - h_{\text{cc}}), \tag{5}$$

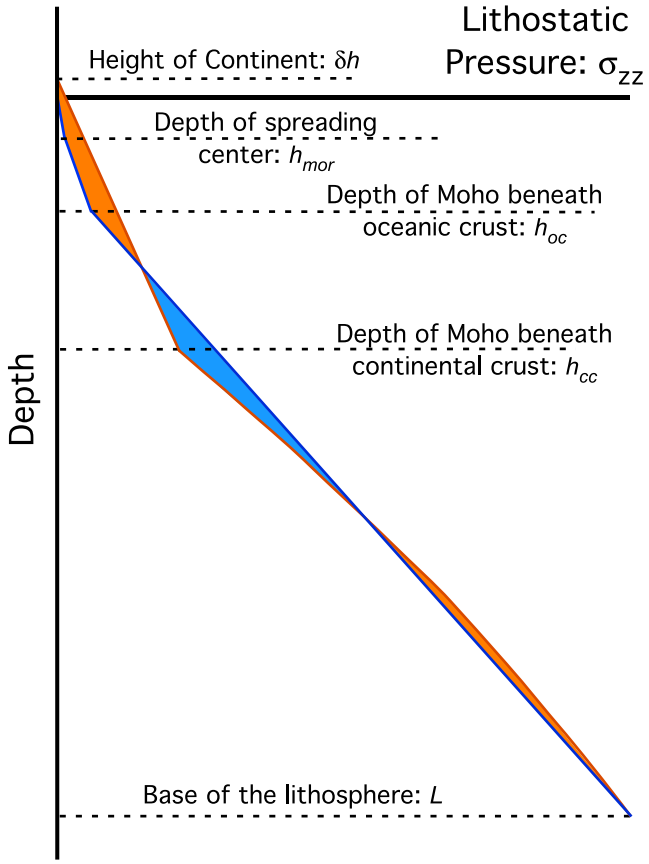

Figure 3. Distorted profiles of lithostatic pressure, σ_{zz} in (8), versus depth beneath continents (orange lines) and spreading centers (blue lines) and differences between them (orange and blue shading). Profiles are distorted in order to show differences, which if plotted to scale would be invisible. As in (7), the value of gravitational potential energy (GPE) for continents is equal to the area between the orange curve and the vertical axis and that for spreading centers equals the area between the blue curve and that axis. For depths greater than L, values of σ_{zz} are presumed to be the same; although integration to greater depth would yield larger values of GPE, the differences between those of continents and spreading centers would not differ. Areas shaded orange show depth ranges in which σ_{zz} beneath continents is greater than that beneath spreading centers, and blue shading shows the opposite. The plot is drawn so that those areas are equal. The difference in GPE, ΔGPE, becomes the difference between the areas of orange and blue shading. Columns could be in isostatic balance, for which σ_{zz} for both columns is the same at the depth L, while values of GPE differed. The surface of the continent is shown above sea level, and σ_{zz} is greater there than beneath the spreading center. Because of thinner oceanic than continental crust, at some depth below the oceanic Moho values of σ_{zz} are equal. The rate that σ_{zz} increases with depth just below the continental Moho is greater than that below the spreading center, because the mantle is the colder there. Because of chemical depletion ($\delta\rho_c(z) = \overline{\delta\rho_c}$), however, the hot, deeper part of the mantle lithosphere beneath continents is slightly less dense than asthenosphere, and σ_{zz} increases more gradually with depth beneath continents than spreading centers.

where $\overline{\delta\rho_c}$ is the mean density anomaly in the mantle due to depletion of iron.

Imposing isostatic balance between the two columns amounts to setting (2) and (5) equal, which can then be expressed, for example, by the following:

$$h_{\mathrm{mor}} = \frac{h_{\mathrm{cc}}(\rho_a - \rho_{\mathrm{cc}}) - h_{\mathrm{oc}}(\rho_a - \rho_{\mathrm{oc}}) - (\frac{1}{2}\,\rho_a\alpha\Delta T_0 - 2\overline{\delta\rho_c})(L - h_{\mathrm{cc}}) - \delta h_c\rho_{\mathrm{cc}}}{\rho_a - \rho_w} \tag{6}$$

An estimate of the depth of spreading centers, h_{mor}, below low continents in Archean time is one target, but obviously, (6) can be rearranged to express different relationships among the various quantities.

The constraint that spreading centers and continental lithosphere were isostatically balanced when thick, cold, Fe-depleted mantle lithosphere had formed requires specification of a minimum of 13 quantities. These include five densities: water (ρ_w), asthenosphere (ρ_a), and averages for oceanic crust (ρ_{oc}), continental crust (ρ_{cc}), and depleted mantle lithosphere beneath continents, or more simply the average difference in densities of asthenosphere and continental lithosphere ($\overline{\delta\rho_c}$). Five depths, thicknesses, or heights must also be specified: depths of water at spreading centers (h_{mor}), the base of the continental lithosphere (L), and the Moho beneath Archean continental crust (h_{cc}), the thickness of oceanic crust (h_{oc}), and the elevation of low continents above sea level (δh). The thickness of continental crust is $h_{\mathrm{cc}} + \delta h$. With the simplest of assumptions that the temperature increases linearly from the Moho to the base of the lithosphere as in (3), two temperatures, T_{Moho} and T_a, and the coefficient of thermal expansion, α, are needed. Thus, isostatic equilibrium, expressed by one equation (6), relates 13 parameters or constrains one parameter when values are assigned to the other 12.

A mathematically precise statement could reduce the number of free parameters by four to yield nine dimensionless quantities. Densities and thicknesses could be scaled to convenient values of each, but because the density of water and the thickness of present-day oceanic crust are known well, such nondimensionalizations gain us little. Because thermal contraction depends on a difference in temperature, combining α with T_a and T_{Moho} yields one dimensionless number: $\alpha(T_a - T_{\mathrm{Moho}})$. Still, the number of quantities that must be specified far exceeds the number of equations that relate them.

One approach to adding constraints, taken by Hynes (2001) and Vlaar (2000), is to assume that melting to form oceanic crust, if not also to deplete the mantle, allows a second equation that relates two densities to one another. Hynes (2001) exploited McKenzie and Bickle (1988) calculations of melt fraction and composition for melting of peridotite, and he obtained curve fits that relate crustal and mantle densities to temperature, T_a. Lambart et al. (2016) pointed out, however, that even if pyroxenite were only 5% of the rock that melts, it can comprise 15% of the melt, which ultimately forms part of the crust. Moreover, as discussed below, suggested thicknesses of Archean oceanic crust range from 7 to 45 km. Thus, I refrain from using such curve fits, except as guides for bounding some densities.

4. GPE per Unit Area as a Constraint on Density Structure

The assumption that the GPE per unit area at spreading centers matches that at low continents adds a second equation that relates the 13 quantities needed to describe isostatic equilibrium and hence a second

constraint. Simply expressed, matching GPE in two columns implies the following:

$$\text{GPE} = \int_{\text{Surface}}^{L} \sigma_{zz}(z)\text{d}z = \text{Constant}, \tag{7}$$

where σ_{zz} is lithostatic pressure, given by the following:

$$\sigma_{zz}(z) = \int_{\text{Surface}}^{z} g\rho(z)\text{d}z \tag{8}$$

and g is gravity (Figure 3). Quantifying potential energy requires choosing a level of zero potential energy, but if isostatic equilibrium holds, then all depths exceeding the depth of compensation yield the same value for the difference in GPE between two regions (e.g., (Molnar & Lyon-Caen, 1988).

A couple of arguments suggest that GPE at spreading centers matches that of continental regions near sea level. Coblentz et al. (1994) and Ghosh et al. (2009) estimated GPE for different regions assuming isostatically compensated density structures. Their work suggests that most differences between GPE of low continents and of spreading centers to be no more than ~1 TN/m. Uncertainties in such calculations are surely that large. More important, GPE scales with geoid height (e.g., Coblentz et al., 2015; Haxby & Turcotte, 1978):

$$\text{GPE} = \frac{g^2}{2\pi G}\Delta N \tag{9}$$

where G is Newton's gravitational constant and ΔN is the geoid height anomaly. A geoid height anomaly of 1 m corresponds to difference in GPE of 0.229 TN/m. The long-wavelength geoid height field reflects mass anomalies in the lower mantle. When they are filtered out, remaining geoid heights over spreading centers and low continents are similar (Coblentz et al., 2015; Doin et al., 1996; Ghosh et al., 2009; Turcotte & McAdoo, 1979). Coblentz et al. (2015) referred to this as the lithospheric geoid. Doin et al. (1996) and Turcotte and McAdoo (1979) used this match of geoid heights to estimate a value of $\overline{\delta\rho_c}$ for stable continents and cratons. Coblentz et al. (2015) and Doin et al. (1996) showed that geoid height anomalies over the mid-ocean ridges and low continents differed little, $\lesssim$2 ($\pm$ ~2) m. Thus, the difference in GPE is ~0.46 TN/m.

The difference in GPE between two regions, ΔGPE, equals the force per unit (horizontal) length that the two regions apply to one another (e.g., Artyushkov, 1973; Dahlen, 1981; Frank, 1972; McKenzie, 1972). Parsons and Richter (1980) referred to this difference as the *driving force* (per unit length): F_l = ΔGPE, and this fact can be used to bound ΔGPE. Dividing F_l by lithospheric thickness, L, gives the vertical average of the horizontal compressive stress, $\overline{\sigma}_{xx}$, that one column of lithosphere applies to the other:

$$\frac{F_l}{L} = \overline{\sigma}_{xx} = \overline{p} + \overline{\tau}_{xx} = 2\overline{\tau}_{xx}, \tag{10}$$

where $\overline{p}$ is the average difference in pressure between the columns and $\overline{\tau}_{xx}$ is the vertically averaged deviatoric compressive stress. The third equality follows from the derivation of the thin viscous sheet equations (e.g.,Bird & Piper, 1980; Dahlen, 1981; England & McKenzie, 1982, 1983; Houseman & England, 1986; Schmalholz et al., 2014), for a balance of GPE underlies the application of a thin viscous sheet to large-scale geodynamics. Consistent with an equality of GPE at spreading centers and low continents, the smaller values of GPE for oceanic lithosphere older than $\gtrapprox$20 Ma accounts for the widespread occurrence of intraplate earthquakes that consistently show thrust faulting (Bergman, 1986; Mendiguren, 1971; Sykes & Sbar, 1973; Wiens & Stein, 1985).

Regarding past time, suppose that GPE for spreading centers and low continents differed. Over a sufficiently long time interval, the resulting force per unit length would deform low continents. For lithosphere, with its low temperature, a description in terms of Newtonian viscosity is obviously a crude approximation, but for the crudeness of calculations here, it suffices. Assuming that $\tau_{xx} = 2\eta\dot{\epsilon}_{xx}$ where η is Newtonian viscosity and $\dot{\epsilon}_{xx}$ is the horizontal compressive strain rate

$$\overline{\dot{\epsilon}}_{xx} = \frac{\Delta\text{GPE}}{4L\eta} = \frac{F_l}{4L\eta} \tag{11}$$

where $\overline{\dot{\epsilon}}_{xx}$ is the vertical average of $\dot{\epsilon}_{xx}$. Among sparse estimates of lithospheric viscosity, Walcott (1970) suggested that $\eta = 1 \times 10^{23}$ Pa s for the Canadian Shield. Gordon and Houseman (2015) estimated

$\tau_{xx} = 40$ GPa and $\dot{\epsilon}_{xx} = 3 \times 10^{-16}$ s^{-1} for old oceanic lithosphere beneath the Indian Ocean, which corresponds to $\eta = 7 \times 10^{22}$ Pa s. England and Molnar (2015) used the difference in GPE and the average strain rate across the Tien Shan to place a lower bound on average viscosity of $\sim 10^{22}$ Pa s. Flesch et al. (2001) and Vergnolle et al. (2007) estimated viscosities of stiffer areas in Asia of $\sim 10^{23}$ Pa s. Turning this around, suppose that a force per unit length of $F_l = 1$ TN/m operated on lithosphere with $L = 200$ km at $\dot{\epsilon}_{xx} \approx 3 \times 10^{-18}$ (or 3×10^{-17}) s^{-1} for 1 Gyr to produce strain of 10% (or ~100%). The average viscosity of the lithosphere would be $\eta \approx 0.5 \times 10^{24}$ (or $\sim 0.5 \times 10^{23}$) Pa s. If crust initially 35 km thick thickened by 3.5 km (or 35 km), and if Airy isostasy held, the surface, initially at sea level, would rise 500 m (or ~5 km). Obviously, continents do not stand so high today, except in special regions that are of limited extent and that have undergone crustal shortening in the past tens of million years. Mean elevations of tectonically quiet continents today lie only ≈200–300 m above sea level (e.g., Harrison et al., 1983). If regions stood so high in Archean time, additional processes must have created larger forces per unit length than can be associated with spreading centers. Alternatively, suppose that a force per unit length of $F_l = -1$ TN/m operated for 1 Gyr. Then crust of low continents would thin and eventually drop below sea level, which is not the case today. Thus, billion-year averages of F_l seem to have been smaller than 1 TN/m. I show below that differences in ΔGPE = ±1 TN/m add little error to estimates of densities and Archean sea level.

This analysis assumes that basal tractions contribute little to the torques that move plates. As is known well, GPE over Tibet is larger than that of mid-ocean ridges, and some have used that difference to argue that basal drag is necessary to sustain India's penetration into the rest of Eurasia (e.g., Ghosh et al., 2006). Sandiford et al. (1995), however, showed that the greater length of the mid-ocean ridge system south of the Indian plate than the length of Tibet compensates for the greater GPE of Tibet than the ridges.

Appendix A presents the requisite algebra that evaluates of GPE at spreading centers and low continents. Balancing them, by setting (A2) and (A11) equal gives, for the case with constant $\delta\rho_c(z) = \overline{\delta\rho_c}$ through the mantle lithosphere

$$\begin{aligned}\frac{1}{2}\rho_a[L^2 - (h_{mor} + h_{oc})^2] + (\rho_w h_{mor} + \rho_{oc} h_{oc})L \\ - \frac{1}{2}\rho_w h_{mor}^2 - \frac{1}{2}\rho_{oc} h_{oc}^2 = \frac{1}{2}\rho_c(h_{cc} + \delta h_c)^2 + \rho_c(h_{cc} + \delta h_c)(L - h_{cc}) \\ + \left(\frac{\rho_a - \overline{\delta\rho_c}}{2}\right)(L - h_{cc})^2 + \left(\frac{\rho_a \alpha \Delta T_0}{3}\right)(L - h_{cc})^2.\end{aligned} \tag{12}$$

For a density deficit that decreases linearly from the Moho to the base of the lithosphere, $\delta\rho_c(z) = 2\overline{\delta\rho_c}(L - z)/(L - h_{cc})$, setting (A2) and (A13) equal gives

$$\begin{aligned}\frac{1}{2}\rho_a\left[L^2 - (h_{mor} + h_{oc})^2\right] + (\rho_w h_{mor} + \rho_{oc} h_{oc})L \\ - \frac{1}{2}\rho_w h_{mor}^2 - \frac{1}{2}\rho_{oc} h_{oc}^2 = \frac{1}{2}\rho_c(h_{cc} + \delta h_c)^2 + \rho_c(h_{cc} + \delta h_c)(L - h_{cc}) \\ + \frac{1}{2}\rho_a(L - h_{cc})^2 + \left(\frac{\rho_a \alpha \Delta T_0 - 2\overline{\delta\rho_c}}{3}\right)(L - h_{cc})^2.\end{aligned} \tag{13}$$

5. Application of Isostasy and GPE to Present-Day Structure

With assumed values of various parameters, equation (6) alone or together with (12) or (13) can be used to constrain the other parameters. Before applying these to Archean conditions, I apply them to the present day, with the goal of placing bounds on values of $\delta\rho_c(z)$ and ρ_{cc} as functions of h_{cc} for present-day conditions. Presumably, their values have not changed since Archean time.

Among the many parameters in (6) and (12) or (13), some are known well: $\rho_w = 1.0 \times 10^3$ kg/m^3, and for the present, $h_{mor} = 2{,}600 \pm 200$ m (e.g.,Crosby & McKenzie, 2009; Hillier & Watts, 2005; Korenaga & Korenaga, 2008) and $h_{oc} = 7$ km (White et al., 1992). As discussed below, I let $\delta h_c = 0$ m. For sensible bounds on the mean density of continental crust, 2.7×10^3 kg/m^3 $\leq \rho_{cc} \leq 3.0 \times 10^3$ kg/m^3. To place bounds on the density of oceanic crust, I exploit Hynes (2001) analysis of McKenzie and Bickle (1988) parameterizations. For the present day, $\rho_{oc} = 3.1 \times 10^3$ kg/m^3, which is approximately what Hynes (2001) inferred for melting sufficient to produce 7 km of crust, but let us consider a range of 3.0×10^3 kg/m^3 $\leq \rho_{oc} \leq 3.2 \times 10^3$ kg/m^3. For the density of

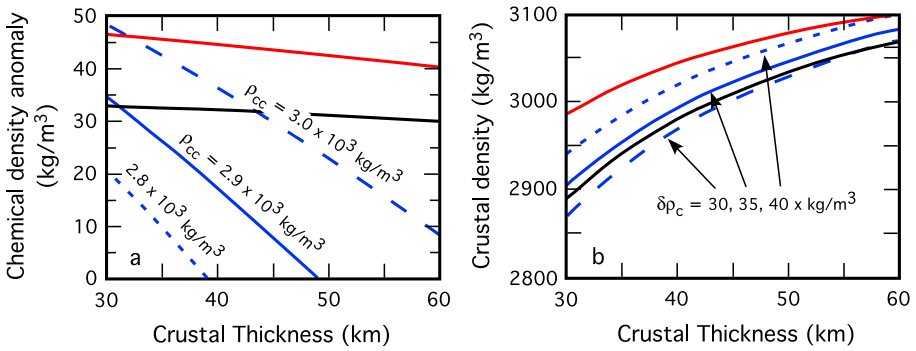

Figure 4. Densities versus thickness of continental crust, h_{cc}: (left) differences in the mean density, $\overline{\delta\rho_c}$, between oceanic and continental lithosphere due to iron depletion and (right) density of continental crust, ρ_{cc}. The black and red lines show $\overline{\delta\rho_c}$ and ρ_{cc} versus h_{cc} for constant values of $\delta\rho_c(z)$ and linearly decreasing values of it, respectively, for cases in which $GPE_{Cont} = GPE_{Ocean}$ with $L = 250$ km, $\rho_{oc} = 3.1 \times 10^3$ kg/m^3, $\rho_a = 3.25 \times 10^3$ kg/m^3, $\delta h_c = 0$ m, and $\alpha(T_a - T_{Moho}) = 0.0315$, where the latter corresponds, for example, to $\alpha = 3.5 \times 10^{-5}$ °C^{-1}, $T_a = 1350$°C, and $T_{Moho} = 450$°C. Blue lines show examples for which only isostatic balance (6) has been assumed. On the left, calculations of $\overline{\delta\rho_c}$ are shown for $\rho_{cc} = 2.8$, 2.9, and 3.0 $\times 10^3$ kg/m^3, and on the right calculated values of ρ_{cc} are shown for density differences between oceanic and continental lithosphere due to iron depletion of $\overline{\delta\rho_c} = 30$, 35, and 40 kg/m^3.

asthenosphere, again following Hynes (2001), $\rho_a = 3.25 \times 10^3$ kg/m^3, but let us allow for 3.2×10^3 kg/m^3 $\leq \rho_a \leq 3.3 \times 10^3$ kg/m^3, though of course, ρ_a must be greater than ρ_{oc}. For continental lithosphere beneath Precambrian terrain, let us consider a range of thicknesses of 200 km $\leq L \leq$ 300 km and of temperatures at the Moho of 350 °C $\leq T_{Moho} \leq$ 550 °C. A present-day value of $T_a = 1350$°C yields $\Delta T = 800 \pm 100$ °C. Finally, for thermal expansivity, a range of 3.0×10^{-5} °C^{-1} $\leq \alpha \leq 4.0 \times 10^{-5}$ °C^{-1} allows for its temperature dependence (e.g., Bouhifd et al., 1996). A range of possible present-day thicknesses, h_{cc}, of Archean crust must be considered, because seismological studies do not show that one value fits all. Although most estimates are in the range of 35 to 40 km, some exceed 50 km (Table 2). To span the observed range, I show calculations for 30 km $\leq h_{cc} \leq$ 60 km.

Figure 4 compares calculated densities with constant values of $\delta\rho_c$ (black lines) throughout the mantle lithosphere with values of it decreasing linearly with depth (red lines), with the same $\overline{\delta\rho_c}$. For columns of mass beneath spreading centers and Archean cratons to be isostatically balanced and for values of GPE to be equal, values of $\overline{\delta\rho_c}$ for linearly decreasing density anomalies are greater than those for constant $\delta\rho_c$ (Figure 4a). A decrease in mass at shallow depths in the mantle lithosphere leads to a decrease in GPE, and therefore, GPE_{Cont} would be the smaller for linearly decreasing $\delta\rho_c$, if the only difference between columns were the depth distribution of $\delta\rho_c$. To compensate for that decrease in GPE_{Cont} while maintaining a balance with GPE_{Ocean}, density must be added to the crust (Figure 4b), but then maintaining isostatic balance requires a compensating

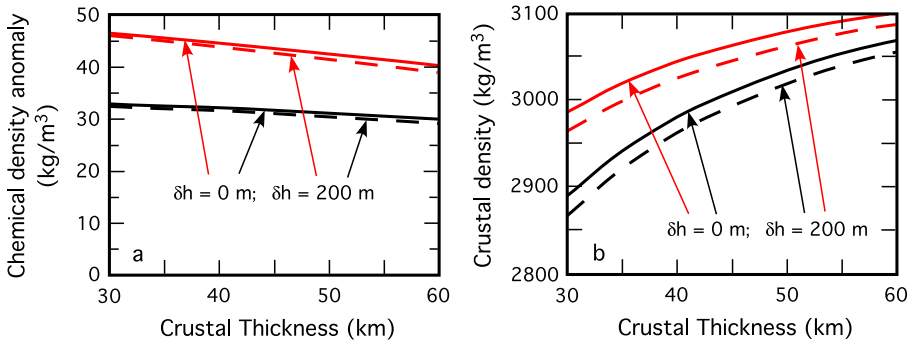

Figure 5. Differences in density, $\overline{\delta\rho_c}$, between oceanic and continental lithosphere due to iron depletion (left) and mean densities of continental, ρ_{cc}, crust versus thickness of continental crust h_{cc} (right), for two values of surface heights of low continents, 0 and 200 m, for both constant values of $\delta\rho_c(z)$ (black lines) and linearly decreasing values of it (red lines). For all curves, $\Delta GPS = 0$, $L = 250$ km, $\rho_a = 3.25$ kg/m^3, $\rho_{oc} = 3.1 \times 10^3$ kg/m^3, and $\alpha(T_a - T_{Moho}) = 0.0315$.

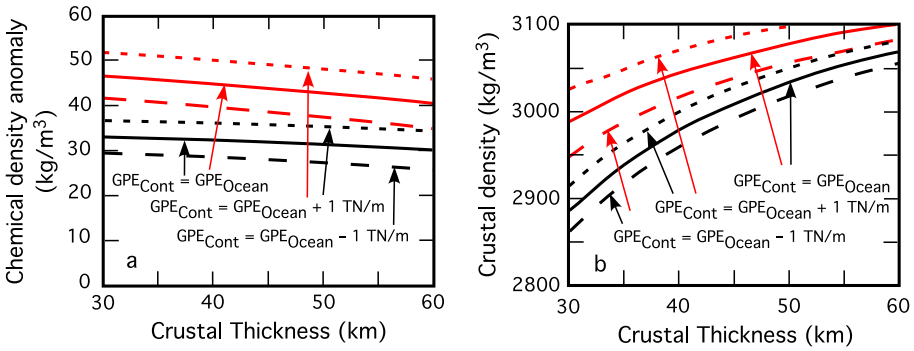

Figure 6. Difference in mean density, $\overline{\delta\rho_c}$, between oceanic and continental lithosphere due to iron depletion (left) and mean density of continental crust, ρ_{cc} (right), versus thickness of continental crust, h_{cc} for different balances of GPE (±1 TN/m) and for different distributions of density deficit, $\delta\rho_c(z)$, in the mantle lithosphere. Black lines show constant values of $\delta\rho_c(z)$, and red lines show values decreasing from $2\overline{\delta\rho_c}$ at the Moho to 0 at the base of the lithosphere. For all curves, L = 250 km, ρ_a = 3.25 kg/m^3, ρ_{oc} = 3.1 ×10^3 kg/m^3, δh_c = 0 m, and $\alpha(T_a - T_{Moho})$ = 0.0315.

reduction in density elsewhere. This is achieved by a greater mean density deficit, $\overline{\delta\rho_c}$ and a greater ρ_{cc}, for linearly decreasing density deficit in the mantle lithosphere than for constant values of it (Figure 4a).

As noted above, balancing GPE for Archean continents and spreading centers adds a constraint that should reduce uncertainties in other parameters. Figure 4 compare inferences of $\overline{\delta\rho_c}$ and ρ_{cc} as functions of h_{cc} based on isostatic balance alone (6) with those using GPE as an additional constraint. Imposing a balance of GPE limits plausible values of both ρ_{cc} and $\overline{\delta\rho_c}$, especially the latter. The black and red lines in Figure 4a show that $\overline{\delta\rho_c}$ depends only weakly on crustal thickness, when ΔGPE = 0, but if constrained only by isostatic balance (blue lines), $\overline{\delta\rho_c}$ depends strongly on the assumed values of ρ_{cc} and h_{cc}. The underlying logic is simple: If crust is made denser, isostasy requires a less dense mantle lithosphere, and hence a larger value of $\overline{\delta\rho_c}$, but a more dense crust and less dense mantle lithosphere increases the GPE of continental lithosphere. To balance GPE, $\overline{\delta\rho_c}$ and ρ_{cc} must trade off sensitively with one another.

The assumed present-day elevation of low continents above sea level, δh_c has little effect on calculated densities (Figure 5). For values of δh_c = 0 and 200 m, calculated vales of $\overline{\delta\rho_c}$ differ by 1–2 kg/m^3, a negligible amount. Those of ρ_{cc} differ by more, ~20 kg/m^3, but still a small fraction of the ~500-kg/m^3 difference between crust and mantle. Present-day average elevations of low, tectonically inactive continents like Australia or Europe, whose mean elevations are not distorted by active mountain belts, are ~200 m (Harrison et al., 1983). Because depths of Archean spreading centers beneath possibly submerged Archean continents is a target, I assume that δh_c = 0 both today and in Archean time.

The equality $GPE_{Cont} = GPE_{Ocean}$ is an assumption. Figure 6 shows the effect of an imbalance in GPE ~1 TN/m (e.g., Coblentz et al., 1994; Ghosh et al., 2009) on calculations of densities; blue and red lines show cases where $GPE_{Cont} = GPE_{Ocean} \pm 1$ TN/m, respectively. If an imbalance of 1 TN/m in GPE existed, it would lead to a 3- to 5-kg/m^3 error in $\delta\rho_c$ and a 25- to 40-kg/m^3 error in ρ_{cc}, with the larger values characterizing linearly decreasing $\delta\rho_c$ through the mantle lithosphere and with the error in ρ_{cc} the more significant. The greater (or smaller) GPE_{Cont} leads to an increase (or decrease) in crustal density, which, to maintain isostatic balance, requires a compensating decrease (or increase) in mantle density, which, in turn, is accomplished by an increase (or decrease) in the mean density deficit, $\overline{\delta\rho_c}$. The differences in $\overline{\delta\rho_c}$ and ρ_{cc} for imbalance in GPE, if not negligible, are not large.

Let L = 250 km, $\rho_{oc} = 3.1 \times 10^3$ kg/m^3, $\rho_a = 3.25 \times 10^3$ kg/m^3, and $\alpha(T_a - T_{Moho}) = 0.0315$, as in Figure 4. Figure 7 shows how plausible end-member values of these parameters affect inferred values $\overline{\delta\rho_c}$ and ρ_{cc} as functions of h_{cc}. I show these only for constant values of $\delta\rho_c(z)$, because plots for linearly decreasing $\delta\rho_c(z)$ are similar.

Figures 7a and 7b show how assumed present-day thicknesses of Archean lithosphere, L, trade-off with $\overline{\delta\rho_c}$ and ρ_{cc}. Their dependences on L are small: 1 to 5 kg/m^3 for $\overline{\delta\rho_c}$ and less than 25 kg/m^3 for ρ_{cc}.

Figures 7c and 7d show $\overline{\delta\rho_c}$ and ρ_{cc} as functions of h_{cc} for three values of ρ_a: 3.20, 3.25, and 3.30 × 10^3 kg/m^3. Values of $\overline{\delta\rho_c}$ are virtually independent of assumed values of ρ_a (Figure 7c). Although ρ_{cc} differs by

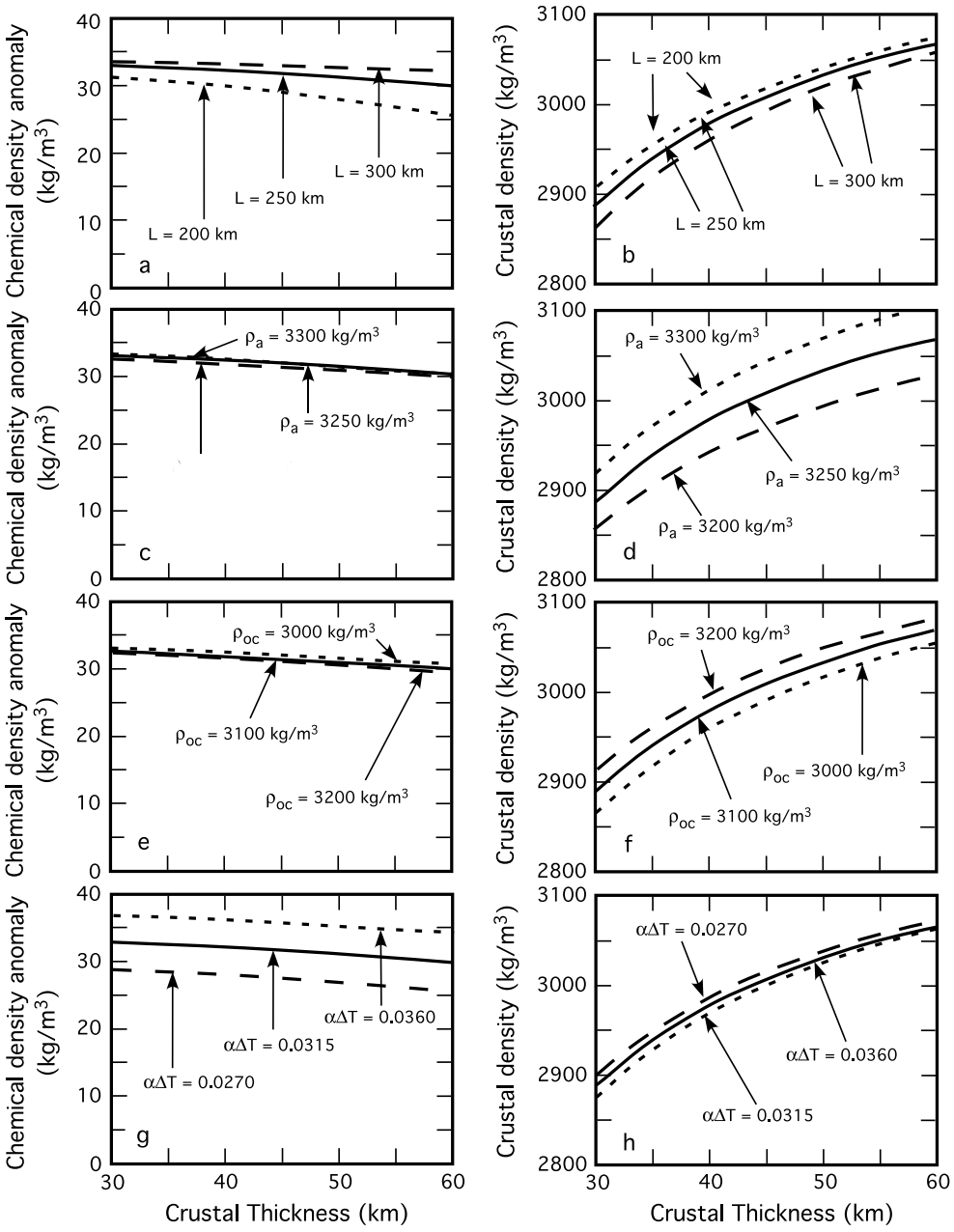

Figure 7. Differences in density, $\overline{\delta\rho_c}$, between oceanic and continental lithosphere due to iron depletion (left) and mean density, ρ_{cc}, of continental crust (right) versus thickness of continental crust h_{cc}, for three values of lithospheric thickness, L (a and b), three values of density of asthenosphere, ρ_a (c and d), three values of density of oceanic crust, ρ_{oc} (e and f), and three values of the product $\alpha(T_a - T_{Moho})$ (g and h). Values of $\alpha(T_a - T_{Moho}) = 0.0270$, 0.0315, and 0.0360 correspond, for example, to $(T_a - T_{Moho}) = 900$ °C, with $\alpha = 3.0$, 3.5, and 4.0 $\times 10^{-5}$ °C^{-1}, respectively. All solid curves correspond to $L = 250$ km, $\rho_a = 3.25$ kg/m^3, $\rho_{oc} = 3.1 \times 10^3$ kg/m^3, and $\alpha(T_a - T_{Moho}) = 0.0315$, and in all cases, the assumed mean height of low continents above sea level is $\delta h_c = 0$ m.

~30–50 kg/m^3 for different ρ_a (Figure 7d), the density contrast at the Moho, $\rho_a - \rho_{cc}$, turns out to be relatively independent of ρ_a. Thus, isostatic balance is achieved similarly for all values of ρ_a.

Figures 7e and 7f show $\overline{\delta\rho_c}$ and ρ_{cc} as functions of h_{cc} for three values of ρ_{oc}: 3.0, 3.1, and 3.2 $\times$ 10^3 kg/m^3. Again $\overline{\delta\rho_c}$ is virtually independent of ρ_{oc}. Although ρ_{cc} differs by 20–30 kg/m^3 for different values of ρ_{oc}, such differences are not large and well within uncertainties of estimates of both.

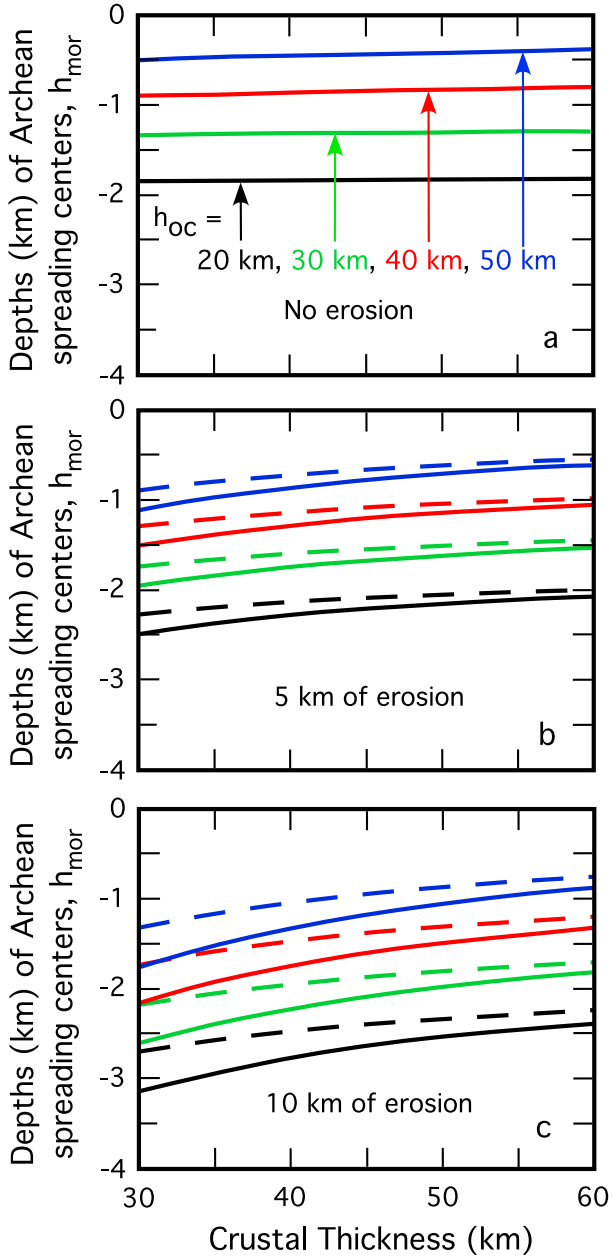

Figure 8. Archean depths of spreading centers below low continents, h_{mor}, versus present-day thickness of continental crust, h_{cc}, for thicknesses of oceanic crust of h_{oc} = 20 km (black), 30 km (green), 40 km (red), and 50 km (blue), for (a) no post-Archean erosion, (b) 5 km of such erosion, and (c) 10 km of erosion. Solid lines show calculated depths, h_{cc}, for constant differences in the mean density, $\delta\rho_c(z)$, between oceanic and continental lithosphere due to iron depletion, and dashed lines show cases with linearly decreasing values of $\delta\rho_c(z)$ through the lithosphere. Other parameters are L = 250 km, $\rho_a = 3.25 \times 10^3$ kg/m^3, $\rho_{oc} = 3.1 \times 10^3$ kg/m^3, and $\alpha = 3.5 \times 10^{-5}$ °C^{-1}. Inferred values of ΔT are nearly independent of and within a few degrees Celsius of the following average values: for no erosion and for h_{oc} = 20 km, 880 °C; 30 km, 853 °C; 40 km, 815 °C; and 50 km, 763 °C. For 5 km of erosion, they are for h_{oc} = 20 km, 906 °C; 30 km, 879 °C; 40 km, 843 °C; and 50 km, 794 °C. For 10 km of erosion, they are for h_{oc} = 20 km, 935 °C; 30 km, 909 °C; 40 km, 873 °C; and 50 km, 828 °C.

Figures 7g and 7h show $\overline{\delta\rho_c}$ and ρ_{cc} as functions of h_{cc} for three values of $\alpha(T_a - T_{Moho})$: 0.270, 0.315, and 0.360, which correspond, for example, to α = 3.0, 3.5, and 4.0 $\times 10^{-5}$ °C^{-1} with T_a = 1350°C and T_{Moho} = 450 °C so that ΔT = 900°C. Among all of Figure 7, values of $\overline{\delta\rho_c}$ depend most on the degree of thermal contraction, for which they span a range of ~10 kg/m^3 (Figure 7g). The strong dependence of $\overline{\delta\rho_c}$ on $\alpha(T_a - T_{Moho})$ should be no surprise, however, given that they trade off against one another in compensating for mass in the mantle lithosphere of Archean regions. Because of this marked dependence, when considering Archean conditions, I explore a range of possible values of $\alpha(T_a - T_{Moho})$. By contrast, the density of the continental crust depends weakly on $\alpha(T_a - T_{Moho})$ and differs from the mean by less than 10 kg/m^3 (Figure 7h).

Figure 4 shows that the assumption of equal GPE per unit area for low continents and spreading centers tightens constraints on ρ_{cc} and $\overline{\delta\rho_c}$. Although uncertainties from ignorance of the other parameters remain, Figures 5–7 show that they contribute small errors to inferred values of ρ_{cc} and $\overline{\delta\rho_c}$. In further analysis, I assume L = 250 km, $\rho_a = 3.25 \times 10^3$ kg/m^3, $\rho_{oc} = 3.1 \times 10^3$ kg/m^3, $\delta h_c = 0$, and $\alpha = 3.5 \times 10^{-5}$ °C^{-1}. Regarding α, laboratory measurements suggest that it depends on temperature, and although a smaller value might be more appropriate for asthenospheric temperatures (Bouhifd et al., 1996), the value of 3.5 $\times 10^{-5}$ °C^{-1} seems an appropriate average for lithospheric conditions (e.g., Schutt & Lesher, 2006).

6. Depths of Archean Spreading Centers Below Low Continents and Moho Temperatures

Presumably, values of ρ_{cc} and $\overline{\delta\rho_c}$ obtained for the present apply to crust and mantle lithosphere in Archean time, but the depth, h_{mor}, of seafloor at spreading centers beneath the level of low continents is likely to have been different from that today, because oceanic crust was thicker than today's ~7 km (Table 3). Writing (12) or (13) as expressions for $\rho_a \alpha \Delta T_0 (L - h_{cc})^2$, and rewriting (6) in terms of $\rho_a \alpha \Delta T_0 (L - h_{cc})$ multiplied by $L_c = L - h_{cc}$ yields pairs of expressions for $\rho_a \alpha \Delta T_0 (L - h_{cc})^2$. Setting them equal and using $L_o = L - h_{oc}$ yields quadratic equations in h_{mor}. For constant $\delta\rho_c(z)$

$$\begin{aligned} 0 = {} & \frac{3}{2}\Delta\rho_w h_{mor}^2 + h_{mor}(3\rho_w L - 3\rho_{oc}h_{oc} - 3\rho_a L_o + 2\Delta\rho_w L_c) \\ & + 3\rho_{oc}(h_{oc}L - \frac{1}{2}h_{oc}^2) + \frac{3}{2}\rho_a(L_o^2 - L_c^2) - \frac{3}{2}\rho_{cc}h_{cc}^2 - 3\rho_{cc}h_{cc}L_c \\ & - 2\Delta\rho_c L_c h_{cc} + 2\Delta\rho_o L_c h_{oc} - \frac{1}{2}\overline{\delta\rho_c}L_c^2 \end{aligned} \tag{14}$$

and for linearly decreasing $\delta\rho_c(z)$

$$\begin{aligned} 0 = {} & \frac{3}{2}\Delta\rho_w h_{mor}^2 + h_{mor}(3\rho_w L - 3\rho_{oc}h_{oc} - 3\rho_a L_o + 2\Delta\rho_w L_c) \\ & + 3\rho_{oc}(h_{oc}L - \frac{1}{2}h_{oc}^2) + \frac{3}{2}\rho_a(L_o^2 - L_c^2) - \frac{3}{2}\rho_{cc}h_{cc}^2 - 3\rho_{cc}h_{cc}L_c \\ & - 2\Delta\rho_c L_c h_{cc} + 2\Delta\rho_o L_c h_{oc} - \frac{2}{3}\overline{\delta\rho_c}L_c^2. \end{aligned} \tag{15}$$

The smaller of the two roots of h_{mor} in (14) or (15) matches current conditions for h_{mor} = 7 km. Plugging values of h_{mor} into (6) (or equivalently (12) or (13) yields an estimate of temperature differences between the asthenosphere and the Moho, $T_a - T_{Moho}$, for continental regions, again as functions of the depth to the Moho below low continents.

Calculations of h_{mor} from (14) or (15) appropriate for Archean time quantify results that ought not be qualitatively surprising (Figure 8a). First, depths of spreading centers below low continents decrease with assumed thickness for Archean oceanic crust. Thicknesses of Archean oceanic crust of 20, 30, 40, and 50 km (Figure 8a) imply less mass in the lithospheric column than today, and that deficit must be compensated by more mass elsewhere. A shallower depth of spreading centers accomplishes that compensation without affecting GPE much (Figure 8a). Note that thicknesses of oceanic crust of 40 or 50 km exceed those for most Archean cratons, but spreading centers still lie deeper than surfaces low continents, even if all oceanic crust is so thick.

Calculated depths of Archean spreading centers in Figure 8a do not depend on how the chemical depletion of the lithosphere is distributed through it, but these calculations have ignored erosion since Archean time. Present-day crustal thicknesses are minimum values for those appropriate for the Archean Eon. Estimated average amounts of erosion for many Archean terrains, however, are not large. Galer and Metzger (1998)

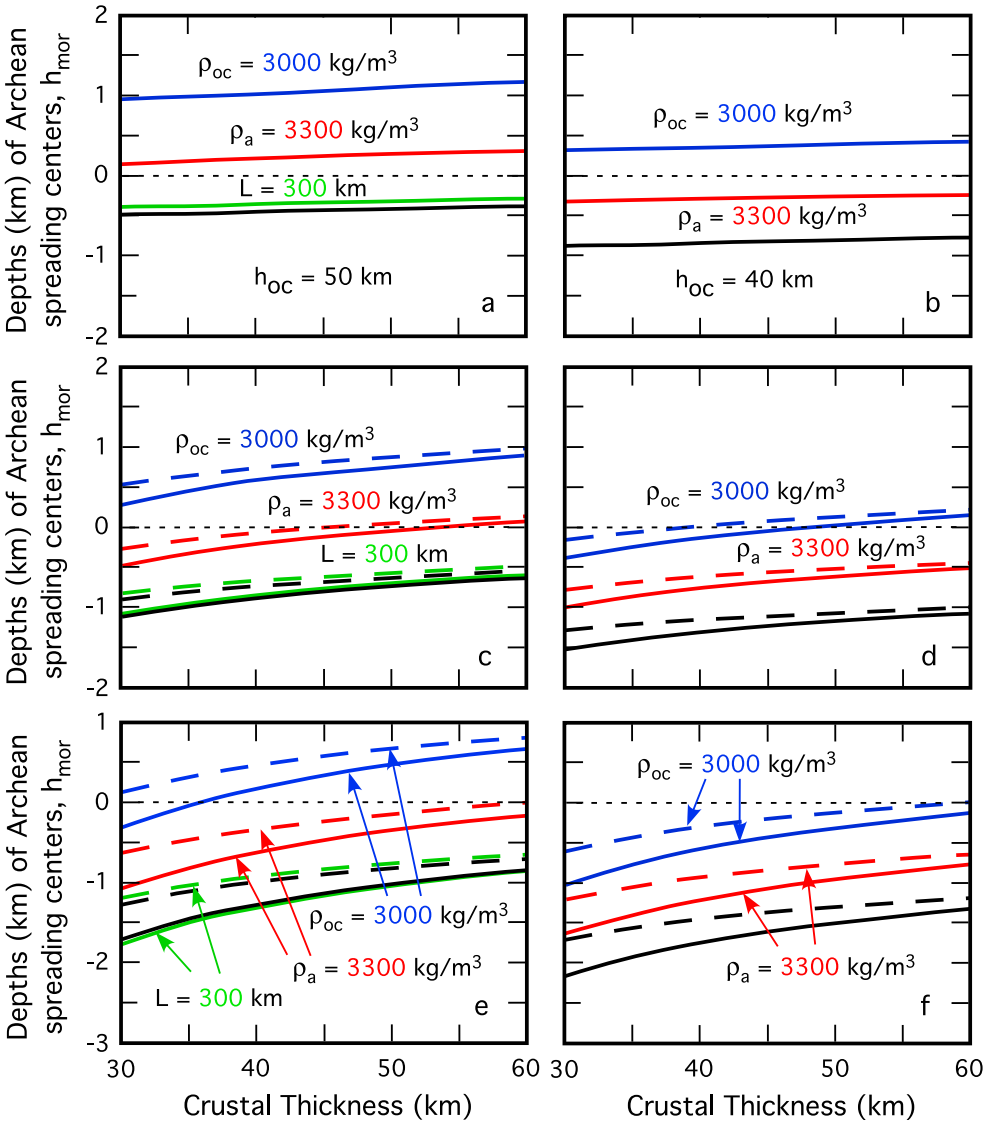

Figure 9. Effects of low-density oceanic crust ρ_{oc} (=3.0 not 3.1 $\times 10^3$ kg/m^3: blue lines), high-density asthenosphere ρ_a (=3.3 not 3.25 $\times 10^3$ kg/m^3: red lines), and thick lithosphere L (=300, not 250 km: green lines) on calculated depths, h_{mor}, of Archean spreading centers below low continents versus thickness of continental crust, h_{cc} for (a and b) no erosion, (c and d) 5 km of erosion, and (e and f) 10 km of erosion, for h_{cc} = 50 km (a, c, and e) and 40 km (b, d, and f). Black lines show cases with L = 250 km, $\rho_{oc} = 3.1 \times 10^3$ kg/m^3, and $\rho_a = 3.25 \times 10^3$ kg/m^3. Solid and dashed lines distinguish calculations for constant $\delta\rho_c(z)$ and linearly decreasing $\delta\rho_c(z)$, respectively. In all cases, $\alpha = 3.5 \times 10^{-5}$ °C^{-1}. Because the effect of different values of L is small, we show it only for h_{cc} = 50 km (left column).

reported that 5 ± 2 km have been eroded from Archean terrains since ~3.0 Ma. From cooling of rock at the surface, Blackburn et al. (2012) inferred that low average erosion rates since 2 Ga, ≲2.5 m/Myr, corresponding to ≲5 km of erosion since 2 Ga. If extrapolated to 3.5 Gyr, erosion since that time would be ≲9 km. Accordingly, Figures 8b and 8c show calculations of h_{mor} from (14) and (15) that allow for removal of 5 and 10 km of Archean continental crust, again using values of ρ_{cc} and $\delta\rho_c$ as functions of crustal thickness beneath low continents deduced for present-day conditions. This assessment of limited erosion ignores evidence of deeply exhumed Archean rock (e.g., Bickle et al., 1980; Boak & Dymek, 1982; England & Bickle, 1984; Grambling, 1981; Perkins & Newton, 1981). Deeply exhumed Archean rock might, however, have risen to the surface by geodynamic processes, such as along low-viscosity channels adjacent to subduction zones, or just thrust faults, as ultrahigh-pressure rock from younger collision zones seems to require (e.g., England & Holland, 1979). In any case, exhumation of deep Archean rock does not seem to be widespread (e.g., Sengör, 1999).

For removal of 5 or 10 km of crust since Archean time, calculated depths of spreading centers below low continents are deeper than if no erosion had occurred (Figure 8a), by ~400–700 m (Figure 8b) or ~600–1,400 m (Figure 8c), respectively. For these cases, the calculated depths of spreading centers depend on how chemical depletion is distributed through the Archean lithosphere, with shallower spreading centers (smaller h_{mor}) for linearly decreasing $\delta\rho_c(z)$ than for constant $\delta\rho_c(z)$ through the lithosphere. Because crustal densities are greater for linearly decreasing $\delta\rho_c(z)$, erosion calls for more mass in the Archean lithospheric column than otherwise. Shallower spreading centers compensate for the required greater mass in the oceanic column.

It turns out that calculated temperature differences between the asthenosphere and Moho, $\Delta T = T_a - T_{Moho}$ for the various cases vary little with present-day thicknesses of continental crust, h_{cc}; the caption of Figure 8 lists their ranges. Moreover, such temperatures depend little on the thickness of Archean oceanic crust, h_{oc}, or amounts of erosion. All are in the range of 850–950 °C. With an Archean temperature of the asthenosphere of 1600–1700 °C, these are consistent with inferred temperatures near the Moho of $T_{Moho} \approx 700$–900 °C (Bickle, 1978; Davis et al., 2003; Grambling, 1981; Jaupart & Mareschal, 2015; Johnson et al., 2017; Michaut et al., 2009; Perkins & Newton, 1981; Rey & Coltice, 2008; Rey & Houseman, 2006; Singh, 2015).

A logical question is: for which parameter is its uncertainty sufficiently large that a plausible value might allow Archean spreading centers to have lain at shallower depths than low continents? First, note that if $\delta h = 200$ m were used for the present, calculated depths of Archean spreading centers would be 200–250 m deeper than those calculated for $\delta h = 0$ m, depending on the amount of post-Archean erosion. Thus, the assumed value for δh is not important here. Next, as is obvious in Figure 8, for Archean oceanic crust to have lain farther from the center of the Earth than the surface of low continents, it must have been thick. Accordingly, an exploration of the parameters that might allow emergent spreading centers needs to consider only $h_{oc} = 40$ and 50 km.

Among the parameters required to describe the density structure, the density of oceanic crust, ρ_{oc}, affects depths of spreading centers most (Figure 9). Were $\rho_{oc} = 3.0 \times 10^3$ kg/m^3 with an Archean crustal thickness of $h_{oc} = 50$ km, spreading centers would lie above the level of low continents regardless of how much post-Archean erosion has occurred (Figure 9, left column). For $h_{oc} = 40$ km, the Archean spreading centers could have lain above the level of low continents if subsequent erosion were small (Figure 9b). For isostatic balance with continents, a low density of oceanic crust, especially where thick, requires a compensating increase in mass in the oceanic column; a shallower spreading center, in effect, replaces low-density seawater with more dense asthenosphere. Even for $\rho_{oc} = 3.0 \times 10^3$ kg/m^3 with an Archean crustal thickness of 20 or 30 km, however, the spreading center should have lain below the level of low continents. More importantly, Hynes (2001) calculated densities of oceanic crust, based on McKenzie and Bickle's (1988) empirical relationships among pressure, temperature, and melt fraction do not allow for thick ocean crust with a density of only 3.0×10^3 kg/m^3.

Among other quantities that might allow Archean spreading centers to be shallower than continents, next in importance is the density of the asthenosphere; a value of $\rho_a = 3.3 \times 10^3$ kg/m^3 yields a shallower spreading center than one with $\rho_a = 3.25 \times 10^3$ kg/m^3, but only if Archean oceanic crust was as thick as 50 km and little subsequent erosion has occurred could an Archean spreading center have lain above low continents (Figure 9a). Finally, a thicker lithosphere, $L = 300$ km instead of 250 km, leads to negligibly shallower Archean spreading centers (Figure 9), and that associated with the assumed value of α is yet smaller (not shown).

Even with the unlikely combination of Archean crust as thick as 40–50 km and limited erosion of Archean continents, the calculations in Figures 8 and 9, in conjunction with the work of Hynes (2001), offer little support for the possibility that Archean spreading centers lay at shallower depths than Archean continents.

7. Depths of Archean Spreading Centers and Low Continents Below Sea Level

The preceding discussion concerns the depths of spreading centers below low continents. Implicit in that discussion is the assumption that sufficient water filled the ocean to the edge of the continent. If the volume of water filling the ocean were small enough, however, spreading centers might have been emergent, even if they lay closer to the center of the Earth than the surfaces of continents. Correspondingly, if the ocean floor away from the spreading centers were sufficiently deep, or if the extent of continental regions were much smaller than that today, the spreading centers might have been emergent (Figure 11).

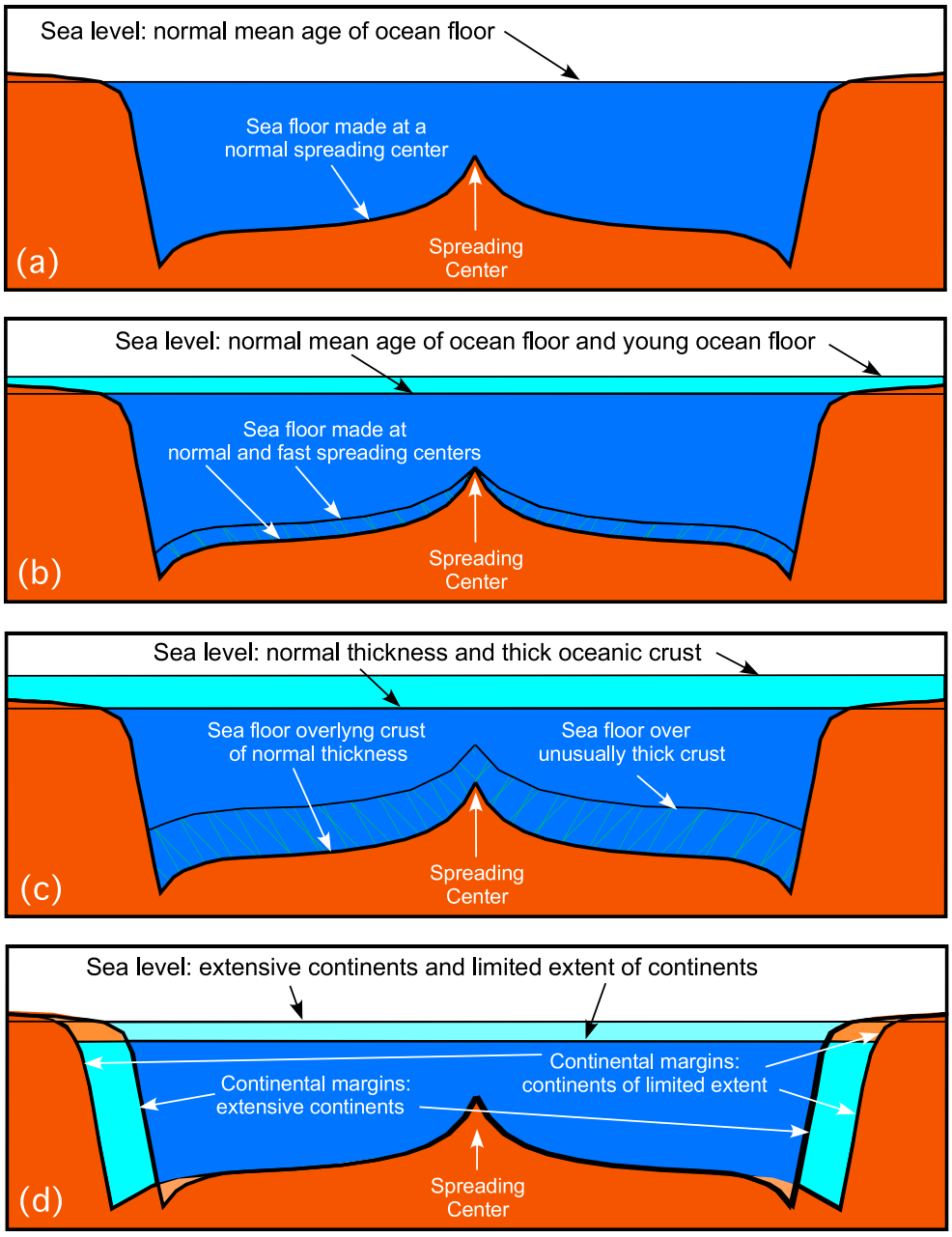

Figure 10. Cartoons of depths of the ocean floor and corresponding sea level. (a) Basic structure with rock shown as brown, and water as blue, with a spreading center, symmetric trenches adjacent to continents, and the sea lapping onto the edge of the continent. (b) The effect of younger ocean floor, denoted by green striping. Because the seafloor is shallower, sea level relative to the continent is higher. (c) The effect of thick oceanic crust, which makes for shallower seafloor everywhere (again shown by green striping), and again for which water laps onto the continents. (d) The effect of less continent, as was the case in early Archean time, and hence a greater volume of the ocean basin. With all else equal, sea level is lower.

Like de Wit and Hynes (1995), Galer (1991), Lee et al. (2017), and Sim et al. (2016), I address this possibility by considering how different temperatures of the asthenosphere, different fractions of area occupied by continents, and different mean ages of oceanic lithosphere affect depths of spreading centers below sea level.

Appendix B develops the basic mathematics, based on work of Parsons (1982) and Parsons and Sclater (1977) and used subsequently by others. It culminates in (B10), which relates the volume of the ocean basin to the area of the ocean (A_0), the depth of spreading centers (h_{mor}), and various thermal parameters including most

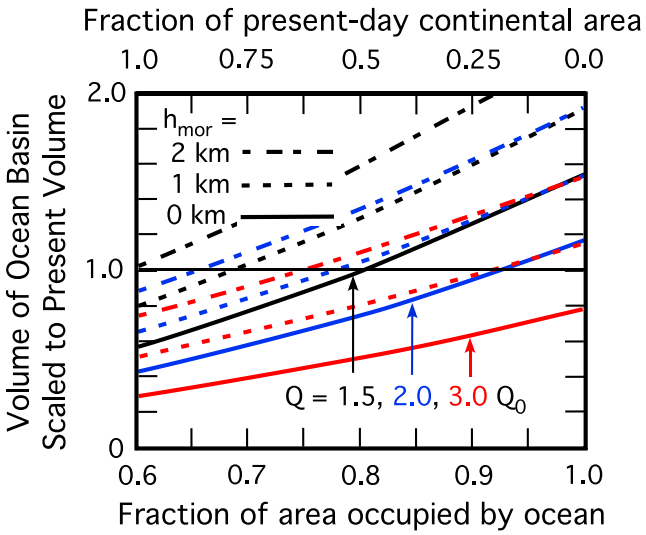

Figure 11. Volumes of ocean basins scaled to that today, as a function of the fraction of the Earth's surface occupied by oceanic crust (bottom axis) or equivalently as a function of the fraction of present-day continental area occupied by thick crust in Archean time (top axis). Curves show such volumes for different depths of spreading centers below low continents of 0 km (solid lines), 1 km (short dashed lines), and 2 km (dot-dashed lines), for different amounts of heat loss through oceanic crust: $Q = 1.5Q_0$ (black), $2.0Q_0$ (blue), and $3.0Q_0$ (red), in all cases for $T_a = 1600$°C.

importantly the heat loss through the ocean floor and the Moho of continental regions (Q):

$$V_0 = A_o\left(h_{\text{mor}} + \frac{64akT_aA_o}{45Q\sqrt{\pi\kappa}}\right). \quad (16)$$

The first term of (16), or (B10), gives the volume of the basin shallower than spreading centers. The second term, which takes into account the mean depth as a function of the mean age of oceanic crust, gives the contribution from the deeper part. Because a, defined in (B4), is proportional to T_a, the second term, scales with T_a^2 (e.g., Galer, 1991; Lee et al., 2017). If heat loss through the oceanic crust, Q, were relatively large, so that ocean floor, on average, were relatively young, the volume of the ocean basin, V_0, would be relatively small. Thus, even for an Archean volume of seawater no greater than that today, the ocean might have spilled onto and covered the continents (Figure 10b).

Volumes of ocean basins given by (16) for different assumed values of depths of spreading centers below low continents, h_{mor}, may be compared with the volume of the present-day ocean ($V_w = 1.36 \times 10^9$ km^3 equal to the sum of the volume of present-day oceans, 1.335×10^9 km^3 (Eakins & Sharman, 2010) and 2.53×10^7 km^3 of ice (Harrison, 1988)), or with yet more seawater as some presume for Archean time. The fraction of the Earth's surface area occupied by deep oceans (not continental shelves) today is ~0.6 but may have shrunk since Archean time, as continents grew. So I consider a range of 0.6 to 1.0 for the fraction of the Earth's surface area occupied by deep oceans (Figure 11). With a smaller Archean areal extent of continents than today (Figure 1), and therefore with a greater areal extent of deep oceans, the volume of Archean ocean basins would have been yet greater than that today (Figures 10 and 11).

The nature of oceanic crust adds an additional complication here. If crust as thick as 30 km or more were routinely made at spreading centers, then the seafloor everywhere would be relatively shallow but still distinctly deeper than continents. If, however, typical Archean oceanic crust were as thin as 20 km, then oceanic plateaus with thicker crust could displace water in the same way that continental crust does. In terms of sea level calculations, such plateaus would appear as continents. In discussions that follow, I try to allow for this possibility without repeatedly adding disruptive qualifying words.

Heat loss from the Earth, Q, presumably was greater in Archean time than today's $Q_0 = 32 \pm 2$ TW (Jaupart, Labrosse, et al., 2015). As expressed by (B9), greater heat loss implies a younger, shallower seafloor (Figure 10b), which makes a smaller volume of the ocean basin in (16). Thus, whether the volume of ocean basins was greater or smaller than that today depends on all of h_{mor}, Q, T_a, A_o, and the volume of water in the Archean ocean (Figures 10 and 11).

Calculations illustrated by Figures 8 and 9 suggest that with plausible thicknesses of oceanic crust and possible amounts of subsequent erosion, spreading centers would have lain ~0–2 km below low continents. Allowing for $h_{\text{mor}} = 0$, 1, or 2 km in (16) with $T_a = 1600$ °C and different values of Q yields plausible volumes of ocean basins that range from greater than to less than that today (Figure 11). For example, suppose that spreading centers lay at the same level as low continents (solid lines in Figure 11). For heat loss three times that today ($3.0Q_0$, red curve), the volume of the ocean basins would have been smaller than the present-day volume of water, V_w. For heat loss twice that today ($2.0Q_0$, blue curve), the volume of the ocean basins could have been smaller than a volume of water 25% more than today ($1.25V_w$), and for heat loss only 50% more than that today ($1.5Q_0$, black curve), the volume of the ocean basins could have been smaller than a volume of water 60% greater than that today ($1.6V_w$), regardless of how much continent had formed. For these cases, surfaces of continents even of negligible extent would have been submerged. At the opposite extreme, with spreading centers lying 2 km below low continents (long dashed lines in Figure 11), for sufficiently small fractions of continent, volumes of the ocean basins could have exceeded the present-day volume of seawater and larger amounts of it, and continents would have stood high and dry.

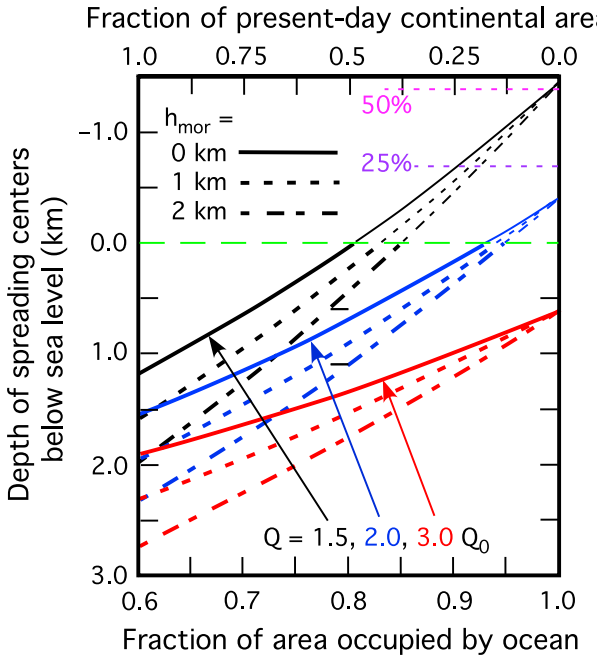

Figure 12. Depths of spreading centers below sea level as a function of the fraction of the Earth's surface occupied by oceanic crust (bottom axis) or equivalently as a function of the fraction of present-day continental area occupied by thick crust in Archean time (top axis). Negative values of h_w in (17) correspond to emergent spreading centers. Curves show such depths below sea level for different depths of spreading centers below low continents of (h_{mor}=) 0 km (solid lines), 1 km (short dashed lines), 2 km (dot-dashed lines), and 3 km (long dashed lines) and for different amounts of heat loss through oceanic crust compared to that of present day: Q = $1.5Q_0$ (black), $2.0Q_0$ (blue) and $3.0Q_0$ (red), in all cases for T_a = 1600°C.

More interesting for Archean conditions than volumes of ocean basins are depths of both spreading centers, h_w, and low continents, h_{lc}, below sea level. For h_w, let us rewrite (16) as follows:

$$h_w = \frac{V_w}{A_o} - \frac{64akT_aA_o}{45Q\sqrt{\pi\kappa}}, \tag{17}$$

where V_w is the volume of seawater and $h_w < 0$ means that spreading centers stand above sea level. The first term (V_w/A_o) gives the average depth of water for an areal extent of oceans of A_o, if the seafloor were flat. The second term takes into account the dependence of the mean depth of the seafloor on its mean age, which scales inversely with heat loss as Q^{-2}. Implicit in (17) is the assumption that water does not spill onto the continents; if volumes of ocean basins were smaller than the volume of water, then water would cover low continents, and (17) would underestimate h_w. The question of interest here, however, is less one of how deep spreading centers may have lain below low continents and more about whether they could have been emergent.

For relatively large heat loss, $Q = 3.0Q_0$, calculations based on (17) do not permit emergent spreading centers ($h_w < 0$), even with an Archean volume of seawater no greater than that today (Figure 12). For less heat loss, however, and for relatively modest amounts of continental crust, spreading centers could have been emergent, especially if the Archean volume of seawater were the same as today. Specifically, for $Q = 2.0Q_0$, if deep oceans occupied $\gtrsim$93–95% of the Earth surface, so that $\lesssim$20% of present-day continental crust had formed, spreading centers, even if 2 km deeper than low continents, could have been emergent. If $Q = 1.5Q_0$, yet more continent could have formed, though no more than one third to perhaps one half of that at present, for spreading centers to have been emergent. With a larger volume of Archean seawater than that today, obviously, conditions allowing emergent spreading centers are more restrictive. In particular, if the volume of Archean seawater were 50% greater than that today, even with continents of limited lateral extent, spreading centers would have been submerged (Figure 12). Finally, for especially thick oceanic crust (40–50 km), for which depths of spreading centers and low continents might have been the same (h_{mor} ~0 km), spreading centers would not have been emergent except for low heat loss.

Next, consider the depths below or heights above sea level at which continents might have lain, again for different depths of spreading centers, h_{mor}, below low continents. We may use (16) to estimate depths, h_{lc}, of water covering low continents. With A_E equal to the surface area of the Earth, the volume of the ocean basin including submerged continents, V_0, is given by

$$V_0 = h_{lc}A_E + \left(h_{mor} + \frac{64akT_mA_o}{45Q\sqrt{\pi\kappa}}\right)A_o \tag{18}$$

which gives for h_{lc}:

$$h_{lc} = \frac{V_0}{A_E} - \left(h_{mor} + \frac{64akT_mA_o}{45Q\sqrt{\pi\kappa}}\right)\frac{A_o}{A_E}. \tag{19}$$

Some simple, not surprising, patterns are clear. Obviously, with a greater Archean than present-day volume of seawater, more continent would be submerged (Figure 13). With smaller fractions of continental crust than today, and hence greater extents of deep oceans, volumes of ocean basins would have been larger (Figures 10d and 11). Thus, when continents had not yet grown to large extents, they would have been more likely to have been emergent than when large expanses of continents had formed, unless oceanic plateaus were widespread (Figure 13). This applies especially when heat loss was small, and ocean basins would have been relatively deep. For $Q = 1.5Q_0$, h_{mor} = 1 km, and an Archean volume of seawater equal to that today, continents could have been emergent, if deep oceans covered ~80% or more of the surface, and correspondingly, only half or less of today's continental extent had formed. By contrast, if Archean oceanic crust were

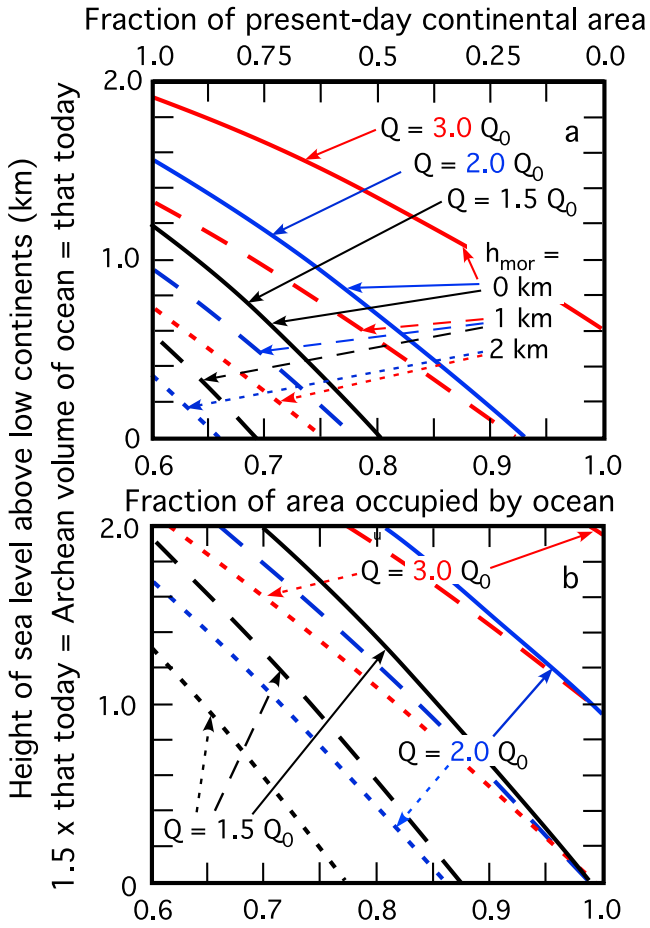

Figure 13. Height of sea level above low continents in Archean time, as a function of the fraction of the Earth's surface occupied by oceanic crust (bottom axis) or equivalently as a function of the fraction of present-day continental area occupied by thick crust in Archean time (top axis), for Archean volumes of seawater equal to (a) and 50% greater than (b) that today, for different amounts of heat loss through oceanic crust compared to that of present day: $1.5Q_0$ (black), $2.0Q_0$ (blue), and $3.0Q_0$ (red), and for different depths (h_{mor} =) 0 km (solid), 1 km (dashed), and 2 km (dot dashed) of spreading centers below low continents. In all cases T_a = 1600°C.

sufficiently thin that spreading centers lay 2 km closer to the center of the Earth than surfaces of low continents (h_{mor} = 2 km), Archean continents could have been emergent under several scenarios (Figure 13): with present-day extents of thick crust (including small continents and vast oceanic plateaus) and deep oceans for $Q = 1.5Q_0$, and for fractions of the Earth covered by deep oceans (a) of $\gtrsim$66% (with $\lesssim$95% of present-day crust) for $Q = 2Q_0$ or (b) of $\gtrsim$75% covered by deep ocean (with $\lesssim$60% of present-day crust) for $Q = 3Q_0$ (Figure 13a). If the Archean volume of seawater were 50% greater than that today, however, and heat loss were $Q = 3.0Q_0$, emergent continents seem virtually impossible (Figure 13b).

8. Discussion

Section 1 noted three topics that bear on depths or exposure of continents and spreading centers in Archean time. First, given geological constraints on the degree to which continental crust had emerged, what limits do such constraints place on the thermal history of the mantle? Second, when might expanses of continental terrain have emerged above sea level, assuming that this was a gradual process that occurred during Archean time? This question bears on some hypotheses for the origin of life. Third, could spreading centers have been emergent in Archean time? This question bears on the temperature of Archean oceans.

8.1. Bounds on the Early Thermal History of the Earth

As reviewed above, evidence of emergent continental crust is sparse for early to middle Archean time but becomes widespread by the Archean-Proterozoic boundary at 2.5 Ga. The inference that emergent continents

were rare, if not virtually absent, at ~3.5 Ga but widespread at ~2.5 Ga can be used to place constraints on the Earth's thermal evolution.

Consider first relatively large heat loss, $Q = 3.0Q_0$, which many consider likely to be appropriate for early Archean time (Davies, 1979, 1980; McKenzie & Weiss, 1975; Richter, 1984, 1985; 1988; Schubert et al., 1980). As shown in Figure 13, low continents would have been submerged (1) if spreading centers lay at the same depths as low continents, $h_{oc} \approx 0$ km, which calls for thick Archean oceanic crust—40–50 km (Figure 8); (2) if $h_{oc} \approx 1$ km, again corresponding to thick oceanic crust, and if more than 20% of continental crust had formed, as many presume (e.g., Abbott & Hoffman, 1984; Armstrong, 1968, 1981; Belousova et al., 2010; Bowring & Housh, 1995; Campbell, 2003; Cawood et al., 2013; DePaolo, 1983; Dhuime et al., 2012, 2015; Hofmann et al., 1986; Kröner, 1985; Pujol et al., 2013; Reymer & Schubert, 1984; Taylor & McLennan, 1995; Wise, 1974; Figure 1); (3) if $h_{oc} \approx 2$ km, corresponding to Archean crustal thicknesses of 20–30 km (Figure 8), and more than 60% of continental crust had formed, or (4) if the volume of Archean seawater were 50% greater than that today. Arguments that a large fraction of continental crust formed during middle Archean time, by 3.5 to 3.0 Ga (Figure 1), are not consistent with both widespread exposure of Archean crust at that time and large heat loss, $Q = 3Q_0$. Conversely, if not only the majority of Archean continental crust had formed when heat loss was $Q = 3Q_0$ but also a significant fraction of that crust was emergent, then Archean spreading centers must have lain at depths below surfaces of continents by $h_{mor} \gtrsim 2$ km (Figure 13), which would then imply that the thickness of Archean oceanic crust was $\lesssim$25 km (Figures 8 and 9).

For late Archean time, 2.5 Ga, much evidence suggests that continental margins, both partly submerged and partly exposed, were widespread. This evidence is consistent with heat loss $Q \approx 2.0Q_0$ (Figure 13), but does not place a tight constraint on the amount of heat loss, because of only weak constraints on the fraction of crust that was emergent or submerged at that time. Suppose $Q(2.5\ \text{Ga}) = 2.0Q_0$ and the volume of water has not changed since 2.5 Ga. Then the blue lines in Figure 13a imply that if late Archean spreading centers were deeper than low continents by (h_{mor}=) 2, 1, or 0 km, surfaces of continents would have lain above sea level, if $\lesssim$85%, $\lesssim$55%, or $\lesssim$20% of present-day continental crust had formed; such fractions correspond to deep oceans covering 66%, 78%, or 93% of the Earth's surface. If the volume of seawater at 2.5 Ga were 50% greater than that today, then emergent continents would require either spreading centers at least ~1 km below low continents or heat loss smaller than $2.0Q_0$ (Figure 13b). If $Q(2.5\ \text{Ga}) = 1.5Q_0$, the existence of emergent continents would be possible even with spreading centers at the same distance from the center of the Earth as low continents, even for 50% more seawater than now. Many have inferred that $\gtrsim$20% of the continental crust had formed by 2.5 Ga (Figure 1); their emergence by 2.5 Ga is consistent with heat loss of $2Q_0$, even with 50% more seawater then than now.

The combination of evidence that much of the Earth's crust had formed by 2.5 Ga (Figure 1) and the calculations in Figure 13 are consistent with late Archean spreading centers lying at least 1 km, and perhaps $h_{mor} >$ 2 km, below the level of low continents. For $h_{mor} > 1$ km, late Archean oceanic crust seems unlikely to have been as thick as 40 km (Figures 8 and 9) and might have been only 20 km thick. If all continental crust had formed by late Archean time (e.g., Armstrong, 1968, 1981; Bowring & Housh, 1995; Wise, 1974), most of it must have been submerged, or heat loss then must have been smaller than $2Q_0$.

8.2. Emergence of Continents and Its Relevance to the Origin of Life

Among hypotheses for the origin of life, some variants of the RNA-first and compartmentalization-first hypotheses call for subaerial, not submarine, environments. (See Appendix C for a brief summary of such hypotheses.) As discussed above, an emergence of land at 3.5 Ga would be allowed only by a subset of plausible heat loss, depths of spreading centers, extents of thick, presumably continental, crust, and volumes of Archean seawater. At one extreme, if Archean oceans contained 50% more water than today, and spreading centers lay at the same elevation as low continents, land would have been submerged regardless of how extensive continents were (Figure 13b). Similarly, for such a volume of Archean seawater, if heat loss were three times that today, $3.0Q_0$, then for continents to have been exposed, spreading centers must have been deeper than ~2 km, which would imply relatively thin Archean oceanic crust, $\lesssim$25 km (Figure 8). At the opposite extreme, if the volume of seawater has changed little since Archean time, and spreading centers lay as deep as 2 km below low continents, then Archean continents could have been emergent: for example, if heat loss were less that $3Q_0$ and $\lesssim$60% of continental crust had formed, or if $Q = 1.5Q_0$ and $\lesssim$85% of continental crust had formed (Figure 13a).

Categorically ruling out emergent early Archean continents, or emergent volcanic plateaus (Kamber, 20102015), seems premature. The weight of opinions, however, that favor relatively thick oceanic crust, $\gtrsim$25 km, and therefore relatively shallow spreading centers, $h_{mor} \lesssim 2$ km (Figure 8), heat loss that exceeded $2Q_0$ in early to middle Archean time, and greater volume of seawater in Archean than present time, render widespread emergent terrain at $\gtrsim$3 Ga unlikely, as others have argued (Arndt, 1999; Ernst et al., 2016; Flament et al., 2008; Lee et al., 2017; McCulloch & Bennett, 1994).

8.3. Emergence of Spreading Centers Above Sea Level?

Oxygen isotopes from Archean marine sediment show unusually large depletion of the heavy isotope (Knauth & Lowe, 2003), and these low δ^{18}O values have elicited three interpretations. (1) The δ^{18}O values do not reflect Archean conditions but instead result from subsequent diagenesis. (2) The Archean ocean was notably warm, 50–80 °C, not like that today (<30 °C; e.g., Knauth, 2005; Knauth & Lowe, 2003; Tartése et al., 2017), an inference supported by analyses of silicon isotopes (Robert & Chaussidon, 2006). (3) Spreading centers were emergent, and subaerial weathering preferentially extracted ^{18}O from the basic crust, so that water entering the ocean would have been depleted in ^{18}O (e.g., Jaffrés et al., 2007; Kasting et al., 2006). Kamber (2010) argued that volcanic provinces, analogous to large igneous provinces of today, were emergent, and weathering of them may have depleted the ocean of ^{18}O. All of de Ronde et al. (1994) from the chemistry of fluid inclusions associated with Archean submarine hot springs, Hren et al. (2009) using both δ^{18}O and δD, and Blake et al. (2010) from δ^{18}O in inorganic phosphate concluded that Archean ocean temperatures were not exceptionally warm, <40 °C. Moreover, using the chemistry of fluid inclusions in rock that formed at 3.2-Ga seafloor hydrothermal vents, de Ronde et al. (1994) placed a lower bound of 982 m on the depth of the ocean overlying these vents, though obviously, this inferred depth applies to only one small segment of diverging oceanic crust in Archean time.

Consistent with inferences drawn by de Wit and Hynes (1995), Galer (1991), and Sim et al. (2016) from assumptions somewhat different from those made here, the results shown in Figure 12 suggest that only in the most extreme of plausible conditions might Archean spreading centers have been emergent. Specifically, if heat loss were $Q = 3.0Q_0$, spreading centers would have been submerged. For no change in the volume of seawater, the extent of thick Archean crust must been less than half that today for $Q = 1.5Q_0$ or <20% of that today for $Q = 2.0Q_0$. For greater Archean than present seawater, continental crust must have been yet less extensive. The idea that subaerial exposure of spreading centers could have contributed to low values of δ^{18}O in Archean seawater (e.g., Jaffrés et al., 2007; Kasting et al., 2006) gains little support.

9. Conclusions

1. The assumption that GPE per unit area stored in continental lithosphere equals that in a column reaching the same depth beneath spreading centers constrains the mean density deficit between mantle lithosphere beneath Archean continents and asthenosphere at the same temperature seems to be 30–35 kg/m^3, if the density deficit is constant through the mantle lithosphere, or 40–45 kg/m^3, if the density deficit decreases linearly through it (Figure 4). These values of $\delta\rho_c$ are similar to others based on petrological arguments (e.g., Arndt et al., 2009; Jordan, 1978; Schutt & Lesher, 2010) and on the geoid (Doin et al., 1996; Turcotte & McAdoo, 1979) but roughly half those proposed by O'Neill et al. (2008) and Poudjom Djomani et al. (2001).
2. Calculated differences in temperatures between the base of the lithosphere and the continental Moho range from 850 to 950 °C. If the asthenosphere were hotter than that at present and with a temperature of ~1600–1700 °C, temperatures at the Moho would have been ~700–900 °C in Archean time.
3. Spreading centers almost surely were not emergent in Archean time, as de Wit and Hynes (1995), Galer (1991), and Sim et al. (2016) inferred, especially if the volume of seawater in Archean time exceeded that today (Figure 12).
4. Emergent Archean continents are permitted by the following conditions (Figure 13): (a) the volume of Archean seawater was not much greater than that today, (b) little continental crust had formed, $\lesssim$20%, as might have been the case in early Archean time (Figure 10d); (c) heat loss from the Earth was closer to twice that today, $2Q_0$, than the more expected $3Q_0$ at 3.5 Ga, so that the mean depth of the ocean floor was not as shallow as it would be with $Q = 3Q_0$ (Figure 10b); and (d) Archean spreading centers lay at least 1 km, and more likely $\gtrsim$2 km, below low continents (Figure 10c). For deep spreading centers, $\gtrsim$2 km below surfaces of low continents, oceanic crust would have been thinner than ~25 km (Figures 8). These conditions seem unlikely and hence do not favor life originating on continental surfaces

5. Conversely, if most, or all, Archean continental crust was submerged at 3.5 Ga, then one of the following seems required: (a) the volume of Archean seawater was greater than that today (Figure 13b); (b) if Archean heat loss was large, $\sim 3Q_0$, $\gtrsim$ 60% of present-day continental crust had formed or oceanic plateaus were widespread, and spreading centers lay $\lesssim$ 2 km below surface of continents (Figure 13a), which implies that Archean oceanic crust was no thinner than ~25 km (Figure 8); (c) if, however, heat loss was not great, $\lesssim 2Q_0$, as seems more likely for late Archean/early Proterozoic time than middle Archean time, again only a fraction of today's volume of crust could have formed, $\lesssim$20%, (i) if Archean spreading centers lay at the same elevation as low continents ($h_{mor} \approx 0$ km), (ii) if $\lesssim$50% of present-day crust had formed with $h_{mor} \approx 1$ km, or (iii) if $\lesssim$85% of present-day crust had formed with $h_{mor} \lesssim 2$ km (Figure 13a).
6. The widespread emergence of Archean crust by 2.5 Ga and the development of continental platforms and shelves are consistent with heat loss roughly twice that today, $2Q_0$. A volume of late Archean continental crust comparable to that today is possible if spreading centers lay 2 km or deeper below low continents, as would be the case if late Archean and early Proterozoic oceanic crust were thinner than ~25 km (Figure 8).

Appendix A: Potential Energy per Unit Area for Continents and Spreading Centers

With g a constant in the upper mantle, the potential energy per unit area for oceanic lithosphere GPE_{oc} can be written as follows:

$$\frac{GPE_{Ocean}}{g} = \int_0^{h_{mor}} \rho_w z dz + \int_{h_{mor}}^{h_{mor}+h_{oc}} (\rho_w h_{mor} + \rho_{oc} z) dz + \int_{h_{mor}+h_{oc}}^{L} (\rho_w h_{mor} + \rho_{oc} h_{oc} + \rho_a z) dz. \tag{A1}$$

Evaluating this and collecting terms leads to

$$\frac{GPE_{Ocean}}{g} = \frac{1}{2}\rho_a[L^2 - (h_{mor} + h_{oc})^2] + (\rho_w h_{mor} + \rho_{oc} h_{oc})L - \frac{1}{2}\rho_w h_{mor}^2 - \frac{1}{2}\rho_{oc} h_{oc}^2. \tag{A2}$$

Determining GPE for continental lithosphere requires an estimate of lithostatic pressure, $\sigma_{zz}(z)$ as function of depth through the crust, $-\delta h_c \le z \le h_{cc}$, and mantle lithosphere. $h_{cc} \le z \le L$. For the crust

$$\frac{\sigma_{zz}(z)}{g} = \rho_{cc}(z + \delta h_c). \tag{A3}$$

If depletion of heavy elements has reduced the density throughout the mantle lithosphere by a constant amount, $\delta\rho_c(z) = \overline{\delta\rho_c}$, then

$$\frac{\sigma_{zz}(z)}{g} = \rho_{cc}(h_{cc} + \delta h_c) + (\rho_a - \overline{\delta\rho_c})z + \rho_a \alpha \int_{h_{cc}}^{z} \Delta T(z) dz. \tag{A4}$$

If instead, density depletion decreased linearly from $2\overline{\delta\rho_c}$ at the Moho to zero at the base of the lithosphere, then with $\delta\rho_c(z) = 2\overline{\delta\rho_c}(L - z)/(L - h_{cc})$:

$$\frac{\sigma_{zz}(z)}{g} = \rho_{cc}(h_{cc} + \delta h_c) + \rho_a z + \int_{h_{cc}}^{z} (\rho_a \alpha \Delta T(z) - \delta\rho_c(z)) dz \tag{A5}$$

Using (5), rewrite (A4) as

$$\frac{\sigma_{zz}(z)}{g} = \rho_{cc}(h_{cc} + \delta h_c) + (\rho_a - \overline{\delta\rho_c})z + \rho_a \alpha \int_{h_{cc}}^{z} \Delta T_0 \frac{L - z}{L - h_{cc}} dz \tag{A6}$$

and (A5) as

$$\frac{\sigma_{zz}(z)}{g} = \rho_{cc}(h_{cc} + \delta h_c) + \rho_a z + \int_{h_{cc}}^{z} (\rho_a \alpha \Delta T_0 - 2\overline{\delta\rho_c}) \frac{L - z}{L - h_{cc}} dz \tag{A7}$$

For the mantle portion of the lithosphere, $h_{cc} \le z \le L$ with constant $\delta\rho_c(z)$:

$$\frac{\sigma_{zz}(z)}{g} = \rho_{cc}(h_{cc} + \delta h_c) + (\rho_a - \overline{\delta\rho_c})z + \rho_a \alpha \Delta T_0 \frac{2L(z - h_{cc}) - (z^2 - h_{cc}^2)}{2(L - h_{cc})} \tag{A8}$$

and with linearly decreasing $\delta\rho_c(z)$:

$$\frac{\sigma_{zz}(z)}{g} = \rho_{cc}(h_{cc} + \delta h_c) + \rho_a z + (\rho_a \alpha \Delta T_0 - 2\overline{\delta\rho_c})\frac{2L(z - h_{cc}) - (z^2 - h_{cc}^2)}{2(L - h_{cc})}. \tag{A9}$$

Inserting (A3) and (A8) into (7) yields the following:

$$\begin{aligned}\frac{\mathrm{GPE_{Cont}}}{g} = &\int_{-\delta h_c}^{h_{cc}} \rho_{cc}(z + \delta h_c)\mathrm{d}z + \int_{h_{cc}}^{L} [\rho_{cc}(\delta h_c + h_{cc}) + (\rho_a - \overline{\delta\rho_c})(z - h_{cc})]\mathrm{d}z \\ &+ \rho_a \alpha \Delta T_0 \int_{h_{cc}}^{L} \frac{2L(z - h_{cc}) - (z^2 - h_{cc}^2)}{2(L - h_{cc})}\mathrm{d}z.\end{aligned} \tag{A10}$$

Evaluating (A10) then gives the following:

$$\begin{aligned}\frac{\mathrm{GPE_{Cont}}}{g} = &\frac{1}{2}\rho_{cc}(h_{cc} + \delta h_c)^2 + \rho_{cc}(h_{cc} + \delta h_c)(L - h_{cc}) \\ &+ (\frac{\rho_a - \overline{\delta\rho_c}}{2})(L - h_{cc})^2 + (\frac{\rho_a \alpha \Delta T_0}{3})(L - h_{cc})^2\end{aligned} \tag{A11}$$

Inserting (A3) and (A9) into (7) yields the following:

$$\begin{aligned}\frac{\mathrm{GPE_{Cont}}}{g} = &\int_{-\delta h_c}^{h_{cc}} c(z + \delta h_c)\mathrm{d}z + \int_{h_{cc}}^{L} [\rho_{cc}(\delta h_c + h_{cc}) + \rho_a(z - h_{cc})]\mathrm{d}z \\ &+ (\rho_a \alpha \Delta T_0 - 2\overline{\delta\rho_c}) \int_{h_{cc}}^{L} \frac{2L(z - h_{cc}) - (z^2 - h_{cc}^2)}{2(L - h_{cc})}\mathrm{d}z.\end{aligned} \tag{A12}$$

Evaluating (A12) then gives the following:

$$\begin{aligned}\frac{\mathrm{GPE_{Cont}}}{g} = &\frac{1}{2}\rho_{cc}(h_{cc} + \delta h_c)^2 + \rho_{cc}(h_{cc} + \delta h_c)(L - h_{cc}) \\ &+ \frac{1}{2}\rho_a(L - h_{cc})^2 + (\frac{\rho_a \alpha \Delta T_0 - 2\overline{\delta\rho_c})}{3})(L - h_{cc})^2.\end{aligned} \tag{A13}$$

Setting $\mathrm{GPE_{Cont}}$ in equation (A11) = $\mathrm{GPE_{Ocean}}$ in equation (A2) yields equation (12), and setting $\mathrm{GPE_{Cont}}$ in equation (A13) = $\mathrm{GPE_{Ocean}}$ in equation (A2) yields equation (13).

Appendix B: Depths of Ocean Floor and Volumes of Ocean Basins as a Function of Age and Heat Loss

Parsons (1982) showed that at present the distribution of area of ocean floor, $A(t)$, as a function of age, t, decreases linearly with t, and updates (e.g., Cogné & Humler, 2004; Rowan & Rowley, 2017; Rowley, 2002) concur with this inference. With the maximum age of t_m, this relationship is given by the following:

$$\frac{\mathrm{d}A(t)}{\mathrm{d}t} = C_0\left(1 - \frac{t}{t_m}\right). \tag{B1}$$

The form of (B1) cannot have applied at all times (e.g.,Labrosse & Jaupart, 2007), but let us presume that deviations have not been significant. Equation (B1) integrates to give

$$A(t) = C_0\left(t - \frac{t^2}{2t_m}\right). \tag{B2}$$

The total area of ocean floor, $A(t_m) = A_o$, has changed since Archean time.

$$A_o = \frac{C_0 t_m}{2}. \tag{B3}$$

Today, for ages $t \lesssim 70$ Ma, the depth of the ocean, $h(t)$, varies with age:

$$h(t) = h_{\text{mor}} + \frac{2\rho_a \alpha T_a}{\rho_a - \rho_w}\sqrt{\frac{\kappa t}{\pi}} = h_{\text{mor}} + at^{\frac{1}{2}} \tag{B4}$$

(e.g., Parsons & Sclater, 1977), where κ is the coefficient of thermal diffusivity. This form does not apply to older seafloor (e.g., Crosby et al., 2006; Hillier, 2010; Hillier & Watts, 2005; Parsons & Sclater, 1977), but with the likelihood that convection was more rapid and heat loss greater in Archean than present time, it seems safe to apply (B4) to Archean seafloor. Moreover, although (B4) is commonly associated with the depth of the seafloor above oceanic lithosphere, the same form applies to the boundary layer of a convecting fluid (Turcotte & Oxburgh, 1967). Thus, the use of (B4) and its derivation do not require that rigid plates participated in horizontal movements in Archean time. Parsons and Sclater (1977) determined that $a = 350$ m/Myr$^{\frac{1}{2}}$, but subsequent refinements with additional data suggest values closer to $a = 320 \pm 20$ m/Myr$^{\frac{1}{2}}$, with $h_r = 2{,}600 \pm 200$ m (Crosby & McKenzie, 2009; Hillier & Watts, 2005; Hoggard et al., 2017; Korenaga & Korenaga, 2008).

The volume of the ocean basin is the integral over age, from $t = 0$ to $t = t_m$, of the product of $h(t)$ and $\mathrm{d}A(t)/\mathrm{d}t$ (Parsons, 1982):

$$V_0 = \int_0^{t_m} h(t)\frac{\mathrm{d}A(t)}{\mathrm{d}t}\mathrm{d}t = \int_0^{t_m} \left(h_{\text{mor}} + at^{\frac{1}{2}}\right) C_0 \left(1 - \frac{t}{t_m}\right) \mathrm{d}t, \tag{B5}$$

where V_0 is the volume of the ocean basin below the level of low continents (not necessarily equal to the volume of seawater). With (B3), (B5) gives

$$V_0 = A_o\left(h_{\text{mor}} + \frac{8at_m^{\frac{1}{2}}}{15}\right) \tag{B6}$$

Obviously, the first term accounts for the volume of the basin shallower than spreading centers, and the second gives the part that is deeper. Again, implicit in (B6) is the assumption that water fills the ocean basin at least to cover spreading centers, so that isostatic compensation includes a depth of water that varies with age of oceanic lithosphere.

Heat flux through oceanic crust, $q(t)$, depends inversely on $\sqrt{t}$ (e.g.,Parsons & Sclater, 1977):

$$q(t) = \frac{kT_a}{\sqrt{\pi\kappa t}}, \tag{B7}$$

where k is the coefficient of thermal conductivity. As with the mean depth, we may calculate the total heat loss, Q, as

$$Q = \int_0^{t_m} q(t)\frac{\mathrm{d}A(t)}{\mathrm{d}t}\mathrm{d}t = \int_0^{t_m} \frac{kT_a}{\sqrt{\pi\kappa t}} C_0 \left(1 - \frac{t}{t_m}\right) \mathrm{d}t. \tag{B8}$$

Evaluating (B8) using (B3) yields the following:

$$Q = \frac{8kT_aA_o}{3}\sqrt{\frac{1}{\pi\kappa t_m}}. \tag{B9}$$

Obviously, t_m varies with Q^{-2} (e.g., Labrosse & Jaupart, 2007).

Inserting (B9) into (B6) yields

$$V_0 = A_o\left(h_{\text{mor}} + \frac{64akT_aA_o}{45Q\sqrt{\pi\kappa}}\right). \tag{B10}$$

As in (B6), the first term of (B10) gives the volume of the basin shallower than spreading centers, and the second, which takes into account the mean depth as a function of mean age of oceanic crust, gives the deeper part.

Appendix C: Hypotheses for the Origin of Life

In simple terms, three views of the origin of life prevail, if with some overlap. In one, sometimes called *metabolism first*, the first key step is for organic molecules to nourish themselves, which in most variants occurs by their extracting protons and moving them across strong gradients in concentration. The leading candidate for the source of protons is Fe from basic and ultrabasic rock that weathers in suboceanic regions (e.g.,Martin & Russell, 2007; Russell & Arndt, 2005; Russell & Hall, 1997; Russell et al., 1988, 1994; Sojo et al., 2016; Wächtershäuser, 1988a, 1988b). Virtually all metabolism-first hypotheses appeal to submarine environments where hot, though not extremely hot, water alters basic rock, which in turn sets up strong proton gradients. The second view, sometimes called the *RNA world*, or *RNA first*, postulates that the first key step is replication, which requires RNA, for RNA not only can store the blueprint for replication but also can both transmit that information and act as a catalyst to create proteins needed for growth (e.g., Benner et al., 1989; Gilbert, 1986; Orgel, 1968; Pressman et al., 2015; Trefil et al., 2009). The third view, the *lipid world* or the *compartmentalization-first* hypothesis, emphasizes the need for cells (enclosed by lipids) to have developed and served as containers that hold replicating organic molecules that can be nourished (e.g., Hanczyc et al., 2003; Powner et al., 2009; Ricardo & Szostak, 2009). Some modern variants of the compartmentalization-first hypothesis include all three of metabolism, replication, and compartmentalization (e.g.,Adamala & Szostak, 2013; Segré et al., 2001; Sutherland, 2016; Szostak, 2011, 2012; Szostak et al., 2001).

Some versions of the RNA-first and compartmentalization-first hypotheses call for subaerial, not submarine, environments. Exposure above sea level would allow exploitation of ultraviolet solar energy not only for destruction of competing processes but more importantly for energy (e.g., Patel et al., 2015; Powner et al., 2009; Szostak, 2009), including possibly photosynthesis (e.g., Benner et al., 1989). Moreover, the land surface would make available particular elements or components that would serve as nutrients (e.g., Mulkidjanian, 2009; Mulkidjanian & Galperin, 2009; Mulkidjanian et al., 2012; Patel et al., 2015; Sutherland, 2016). I take no stand on which of subaerial or submarine settings for the origin of life is correct, but if land must be emergent for either the RNA first or the compartmentalization-first hypothesis to have succeeded, let alone to develop together, the calculations discussed here bear on this question.

Acknowledgments
Philip England reminded me of the equality of gravitational potential energy at mid-ocean ridges and low continents today. He and David Coblentz helped with arguments about geoid heights. England, T. L. Grove, J. E. Johnson, F. A. Macdonald, and B. A. Wing encouraged me to pursue this topic. England, N. Arndt, and an anonymous reviewer offered constructive criticism that improved the logic and presentation. All data are in papers cited, or based on equations in the text.

References

Abbott, D, Burgess, L., Longhi, J., & Smith, W. H. F. (1994). An empirical thermal history of the Earth's upper mantle. *Journal of Geophysical Research*, *99*, 13,835–13,850.

Abbott, D. H., & Hoffman, S. E. (1984). Archaean plate tectonics revisited 1. Heat flow, spreading rate, and the age of subducting oceanic lithosphere and their effects on the origin and evolution of continents. *Tectonics*, *3*, 429–448.

Abe, Y., & Matsui, T. (1988). Evolution of an impact-generated H_2O-O_2 atmosphere and formation of a hot proto-ocean on Earth. *Journal of Atmospheric Sciences*, *45*, 3081–3101.

Adamala, K., & Szostak, J. W. (2013). Nonenzymatic template-directed RNA synthesis inside model protocells. *Science*, *342*, 1098–1100.

Allègre, C. J., & Rousseau, D. (1984). The growth of continents through geological time studied by Nd isotope analysis of shales. *Earth and Planetary Science Letters*, *67*, 19–34.

Allègre, C. J., Staudacher, T., Sarda, P., & Kurz, M. (1983). Constraints on evolution of Earth's mantle from rare gas systematics. *Nature*, *303*, 762–776.

Angus, D. A., Kendall, J.-M., Wilson, D. C., White, D. J., Sol, S., & Thomson, C. J. (2009). Stratigraphy of the Archean western Superior Province from *P*- and *S*-wave receiver functions: Further evidence for tectonic accretion? *Physics of the Earth and Planetary Interiors*, *177*, 206–216.

Armstrong, R. L. (1968). A model for the evolution of strontium and lead isotopes in a dynamic Earth. *Reviews of Geophysics and Space Physics*, *6*, 175–200.

Armstrong, R. L. (1981). Radiogenic isotopes: The case for crustal recycling on a near-steady-state no-continental-growth Earth. *Philosophical Transactions of the Royal Society of London, A*, *301*, 443–472. https://doi.org/10.1098/rsta.1981.0122

Arndt, N. (1999). Why was flood volcanism on submerged continental platforms so common in the Precambrian? *Precambrian Research*, *97*, 155–164.

Arndt, N. T., Coltice, N., Helmstaedt, H., & Gregoire, M. (2009). Origin of Archean subcontinental lithospheric mantle: Some petrological constraints. *Lithos*, *109*, 61–71.

Arndt, N., & Davaille, A. (2013). Episodic Earth evolution. *Tectonophysics*, *609*, 661–674.

Arndt, N. T., & Goldstein, S. L. (1987). Use and abuse of crust-formation ages. *Geology*, *15*, 893–895.

Artyushkov, E. V. (1973). Stresses in the lithosphere caused by crustal thickness inhomogeneities. *Journal of Geophysical Research*, *78*, 7675–7708.

Bank, C. G., Bostock, M. G., Ellis, R. M., & Cassidy, J. F. (2000). A reconnaissance teleseismic study of the upper mantle and transition zone beneath the Archean Slave craton in NW Canada. *Tectonophysics*, *319*, 151–166.

Bedini, R. M., Blichert-Toft, J., Boyet, M., & Albarade, F. (2004). Isotopic constraints on the cooling of the continental lithosphere, Earth Planet. *Science Letters*, *223*, 99–111.

Belousova, E. A., Kostitsyn, Y. A., Griffin, W. L., Begg, G. C., O'Reilly, S. Y., & Pearson, N. J. (2010). The growth of the continental crust: Constraints from zircon Hf-isotope data. *Lithos*, *119*, 457–466.

Benner, S. A., Ellington, A. D., & Tauer, A. (1989). Modern metabolism as a palimpsest of the RNA world. *Proceedings of the National Academy of Sciences of the United States of America*, *86*, 7054–7058.

Bergman, E. A. (1986). Intraplate earthquakes and the state of stress in oceanic lithosphere. *Tectonophysics*, *132*, 1–35.

Beukes, N. J. (1984). Sedimentology of the Kuruman and Griquatown Iron-formations, Transvaal Supergroup, Griqualand West, South Africa. *Precambrian Research*, *24*, 47–84.
Beukes, N. J. (1987). Facies relations, depositional environments and diagenesis in a major early Proterozoic stromatolitic carbonate platform to basinal sequence, Campbellrand Subgroup, Transvaal Supergroup, southern Africa. *Sedimentary Geology*, *54*, 1–46.
Bickle, M. J. (1978). Heat loss from the Earth: A constraint on Archean tectonics from the relation between geothermal gradients and the rate of plate production. *Earth and Planetary Science Letters*, *40*, 301–315.
Bickle, M. J. (1986). Implications of melting for stabilization of the lithosphere and heat loss in the Archaean. *Earth and Planetary Science Letters*, *80*, 314–324.
Bickle, M. J., Bettenay, L. F., Boulter, C. A., Groves, D. I., & Morant, P. (1980). Horizontal tectonic intercalation of an Archaean gneiss belt and greenstones, Pilbara Block, Western Australia. *Geology*, *8*, 525–529.
Bickle, M. J., Martin, A., & Nisbet, E. G. (1975). Basaltic and peridotitic komatiites and stromatolites above a basal unconformity in the Belingwe greenstone belt, Rhodesia. *Earth and Planetary Science Letters*, *27*, 155–162.
Bird, P., & Piper, K. (1980). Plane stress finite element models of tectonic flow in southern California. *Physics of the Earth and Planetary Interiors*, *21*, 58–175.
Blackburn, T. J., Bowring, S. A., Perron, J. T., Mahan, K. H., Dudas, F. O., & Barnhart, K. R. (2012). An exhumation history of continents over billion-tear time scales. *Science*, *335*, 73–76.
Blake, R. E., Chang, S. J., & Lepland, A. (2010). Phosphate oxygen isotope evidence for a temperate and biologically active Archean ocean. *Nature*, *464*, 1029–1032.
Boak, J. L., & Dymek, R. F. (1982). Metamorphism of the ca. 3800 Ma supracrustal rocks at Isua, West Greenland: Implications for early Archaean crustal evolution. *Earth and Planetary Science Letters*, *59*, 155–176.
Borah, K., Rai, S. S., Prakasam, K. S., Gupta, S., Priestley, K., & Gaur, V. K. (2014). Seismic imaging of crust beneath the Dharwar Craton, India, from ambient noise and teleseismic receiver function modelling. *Geophysical Journal International*, *197*, 748–767.
Bouhifd, M. A., Andrault, D., Fiquet, G., & Richet, P. (1996). Thermal expansion of forsterite up to the melting point. *Geophysical Research Letters*, *23*, 1143–1146.
Bowring, S. A., & Housh, T. (1995). The Earth's early evolution. *Science*, *269*, 1535–1540.
Boyd, F. R., & Gurney, J. J. (1986). Diamonds and the African lithosphere. *Science*, *232*, 472–477.
Boyd, F. R., Gurney, J. J., & Richardson, S. H. (1985). Evidence for a 150-200-km thick Archaean lithosphere from diamond inclusion thermobarometry. *Nature*, *315*, 387–389.
Bradley, D. C. (2008). Passive margins through Earth history. *Earth-Science Reviews*, *91*, 1–26.
Brune, J. N., & Dorman, J. (1963). Seismic waves and Earth structure in the Canadian Shield. *Bulletin of the Seismological Society of America*, *53*, 167–210.
Buick, R., Thornett, J. R., McNaughton, N. J., Smith, J. B., Barley, M. E., & Savage, M. (1995). Record of emergent continental crust 3.5 billion years ago in the Pilbara Craton of Australia. *Nature*, *375*, 574–577.
Burke, K., & Kidd, W. S. F. (1978). Were Archean continental geothermal gradients much steeper than those of today? *Nature*, *272*, 240–241.
Campbell, I. H. (2003). Constraints on continental growth models from Nb/U ratios in the 3.5 Ga Barberton and other Archaean basalt-komatiite suites. *American Journal of Science*, *303*(4), 319–351.
Campbell, I. H., & Davies, D. R. (2017). Raising the continental crust. *Earth and Planetary Science Letters*, *460*, 112–122.
Canil, D., Schulze, D. J., Hall, D., Hearn, B. C., & Milliken, S. M. Jr (2003). Lithospheric roots beneath western Laurentia: The geochemical signal in mantle garnets. *Canadian Journal of Earth Sciences*, *40*, 1027–1051.
Carlson, R. W., Boyd, F. R., Shirey, S. B., Janney, P. E., Grove, T. L., Bowring, S. A., et al. (2000). Continental growth, preservation and modification in southern Africa. *GSA Today*, *10*, 1–6.
Carlson, R. W., Pearson, D. G., Boyd, F. R., Shirey, S. B., Irvine, G., Menzies, A. H., & Gurney, J. J. (1999). Re-Os systematics of lithospheric peridotites: Implications for lithosphere formation and preservation. In *Proceedings of the 7th International Kimberlite Conference* (pp. 99–108). Red Roof Design, Cape Town.
Carlson, R. W., Pearson, D. G., & James, D. E. (2005). Physical, chemical, and chronological characteristics of continental mantle. *Reviews of Geophysics*, *43*, RG1001. https://doi.org/10.1029/2004RG000156
Cawood, P. A., Hawkesworth, C. J., & Dhuime, B. (2013). The continental record and the generation of continental crust. *Geological Society of America Bulletin*, *125*, 14–32.
Christensen, U. R. (1984). Heat transport by variable viscosity convection and implications for the Earth's thermal evolution. *Physics of the Earth and Planetary Interiors*, *35*, 264–282.
Christensen, U. R. (1985). Thermal evolution models for the Earth. *Journal of Geophysical Research*, *90*, 2995–3007.
Coblentz, D., Richardson, R. M., & Sandiford, M. (1994). On the gravitational potential of the Earth's lithosphere. *Tectonics*, *13*, 929–945.
Coblentz, D., van Wijk, J., Richardson, R. M., & Sandiford, M. (2015). The upper mantle geoid: Implications for continental structure and the intraplate stress field. In G. R. Foulger, M. Lustrino, & S. King (Eds.), *The Interdisciplinary Earth: A Volume in Honor of Don L. Anderson* (Vol. 514, pp. 197–214). Boulder, CO: Special Paper of the Geological Society of America.
Cogley, J. G., & Henderson-Sellers, A. (1984). The origin and earliest state of the Earth's hydrosphere. *Reviews of Geophysics and Space Physics*, *22*, 131–175.
Cogné, J.-P., & Humler, E. (2004). Temporal variation of oceanic spreading and crustal production rates during the last 180 My. *Earth and Planetary Science Letters*, *227*, 427–739.
Collerson, K. D., & Kamber, B. S. (1999). Evolution of the continents and the atmosphere inferred from Th-U-Nb systematics of the depleted mantle. *Science*, *283*, 1519–1522.
Condie, K. C., & Aster, R. C. (2010). Episodic zircon age spectra of orogenic granitoids: The supercontinent connection and continental growth. *Precambrian Research*, *180*, 227–236.
Crosby, A. G., & McKenzie, D. (2009). An analysis of young ocean depth, gravity and global residual topography. *Geophysical Journal International*, *178*, 1198–1219.
Crosby, A. G., McKenzie, D., & Sclater, J. G. (2006). The relationship between depth, age, and gravity in the oceans. *Geophysical Journal International*, *166*, 553–573.
Dahlen, F. A. (1981). Isostasy and the ambient state of stress in the oceanic lithosphere. *Journal of Geophysical Research*, *86*, 7801–7807.
Darbyshire, F. A., Eaton, D. W., Frederiksen, A. W., & Ertolahti, L. (2007). New insights into the lithosphere beneath the Superior Province from Rayleigh wave dispersion and receiver function analysis. *Geophysical Journal International*, *169*, 10431068. https://doi.org/10.1111/j.1365-246x.2006.03259.x
Das, R., Saikia, U., & Rai, S. S. (2015). The deep geology of South India inferred from Moho depth and Vp/Vs ratio. *Geophysical Journal International*, *203*, 910–926.

Davies, G. F. (1979). Thickness and thermal history of continental crust and root zones. *Earth and Planetary Science Letters*, *44*, 231–238.
Davies, G. F. (1980). Thermal histories of convective Earth models and constraints on radiogenic heat production in the Earth. *Journal of Geophysical Research*, *85*, 2517–2530.
Davis, W. J., Canil, D., MacKenzie, J. M., & Carbno, G. B. (2003). Petrology and U-Pb geochronology of lower crustal xenoliths and the development of a craton, Slave province, Canada. *Lithos*, *71*, 541–573.
de Ronde, C. E. J., de Wit, M. J., & Spooner, E. T. C. (1994). Early Archean (>3.2 Ga) iron-oxide-rich, hydrothermal discharge vents in the Barberton greenstone belt, South Africa. *Geological Society of America Bulletin*, *106*, 86–104.
de Wit, M. J., & Hynes, A. (1995). The onset of interaction between the hydrosphere and oceanic crust, and the origin of the first continental lithosphere. In M. E. Coward & A. C. Ries (Eds.), *Early Precambrian Processes* (pp. 1–9). Boulder, CO: Geological Society Special Publication No. 95.
de Wit, M. J., Roering, C., Hart, R. G., Armstrong, R. A., de Ronde, C. E. J., Green, R. W. E., et al. (1992). Formation of an Archean continent. *Nature*, *357*, 553–562.
de Wit, M. J., & Tinker, J. (2004). Crustal structures across the central Kaapvaal craton from deep-seismic reflection data. *South African Journal of Geology*, *107*, 185–206. Kaapvaal Craton - Special Volume.
DePaolo, D. J. (1983). The mean life of continents: Estimates of continent recycling rates from Nd and Hf isotopic data and implications for mantle structure. *Geophysical Research Letters*, *10*, 705–708.
Debayle, E., & Ricard, Y. (2012). A global shear velocity model of the upper mantle from fundamental and higher Rayleigh mode measurements. *Journal of Geophysical Research*, *117*, B10308. https://doi.org/doi:10.1029/2012JB009288
Delph, J. R., & Porter, R. C. (2014). Crustal structure beneath southern Africa: Insight into how tectonic events affect the Mohorovicic discontinuity. *Geophysical Journal International*, *200*, 254–264.
Dhuime, B., Hawkesworth, C. J., Cawood, P. A., & Storey, C. D. (2012). A change in the geodynamics of continental growth 3 billion years ago. *Science*, *335*, 1334–1336.
Dhuime, B., Wuestefeld, A., & Hawkesworth, C. J. (2015). Emergence of modern continental crust about 3 billion years ago. *Nature Geoscience*, *8*, 552–555.
Doin, M.-P., Fleitout, L., & McKenzie, D. (1996). Geoid anomalies and the structure of continental and oceanic lithospheres. *Journal of Geophysical Research*, *101*, 16,119–16,135.
Drummond, B. J. (2003). Detailed seismic velocity/depth models of the upper lithosphere of the Pilbara Craton, Northwest Australia. *BMR Journal of Australian Geology & Geophysics*, *8*, 35–51.
Eakins, B. W., & Sharman, G. F. (2010). *Volumes of the World's Oceans from ETOPO1*. Boulder, CO: NOAA National Geophysical Data Center. Retrieved from https://www.ngdc.noaa.gov/mgg/global/etopo1_ocean_volumes.html
England, P., & Bickle, M. (1984). Continental thermal and tectonic regimes during the Archean. *Journal of Geology*, *92*(4), 353–367.
England, P. C., & Holland, T. J. B. (1979). Archimedes and the Tauern eclogites: The role of buoyancy in the preservation of exotic eclogitic blocks. *Earth and Planetary Science Letters*, *44*, 287–294.
England, P. C., & Houseman, G. A. (1989). Extension during continental convergence, with application to the Tibetan Plateau. *Journal of Geophysical Research*, *94*, 17,561–17,579.
England, P., & McKenzie, D. (1982). A thin viscous sheet model for continental deformation. *Geophysical Journal Royal Astronomical Society*, *70*, 295–321.
England, P., & McKenzie, D. (1983). Correction to: A thin viscous sheet model for continental deformation. *Geophysical Journal Royal Astronomical Society*, *73*, 523–532.
England, P., & Molnar, P. (2015). Rheology of the lithosphere beneath the central and western Tien Shan. *Journal of Geophysical Research: Solid Earth*, *120*, 3803–3823. https://doi.org/doi:10.1002/2014JB011733
Eriksson, P. G., Mazumder, R., Catuneanu, O., Bumby, A. J., & Ountsché Ilondo, B. (2006). Precambrian continental freeboard and geological evolution: A time perspective. *Earth-Science Reviews*, *79*, 165–204.
Ernst, W. G., Sleep, N. H., & Tsujimori, T. (2016). Plate-tectonic evolution of the Earth: bottom-up and top-down mantle circulation. *Canadian Journal of Earth Sciences*, *53*(11), 1103–1120.
Fitton, J. G., & Godard, M. (2004). Origin and evolution of magmas on the Ontong Java Plateau. In J. G. Fitton, J. J. Mahoney, P. J. Wallace, & A. D. Saunders (Eds.), *Origin and Evolution of the Ontong Java Plateau* (pp. 151–178). London: Geological Society of London Special Publication 229. https://doi.org/10.1144 /GSL.SP.2004.229.01.10
Flament, N., Coltice, N., & Rey, P. F. (2008). A case for late-Archaean continental emergence from thermal evolution models and hypsometry. *Earth and Planetary Science Letters*, *275*, 326–336.
Flesch, L. M., Haines, A. J., & Holt, W. E. (2001). Dynamics of the India-Eurasia collision zone. *Journal of Geophysical Research*, *106*, 16,435–16,460.
Frank, F. C. (1972). Plate tectonics, The analogy with glacier flow, and isostasy. In *Flow and Fracture of Rocks, The Griggs Volume, Geophysical Monograph Flow and Fracture of Rocks, The Griggs Volume, Geophysical Monograph 16* (pp. 285–292). Washington, DC: American Geophysical Union.
Fyfe, W. S. (1978). Evolution of the Earth's crust: Modern plate tectonics to ancient hot spot tectonics. *Chemical Geology*, *23*, 89–114.
Galer, S. J. G. (1991). Interrelationships between continental freeboard, tectonics and mantle temperature. *Earth and Planetary Science Letters*, *105*, 214–228.
Galer, S. J. G., & Metzger, K. (1998). Metamorphism, denudation and sea level in the Archean and cooling of the Earth. *Precambrian Research*, *92*, 389–412.
Ganne, J., & Feng, X.-j. (2017). Primary magmas and mantle temperatures through time. *Geochemistry, Geophysics, Geosystems*, *18*, 872–888. https://doi.org/doi:10.1002/2016GC006787
Ghosh, A., Holt, W. E., & Flesch, L. M. (2009). Contribution of gravitational potential energy differences to the global stress field. *Geophysical Journal International*, *179*, 787–812. https://doi.org/10.1111/j.1365-246x.2009.04326.x
Ghosh, A., Holt, W. E., Flesch, L. M., & Haines, A. J. (2006). The gravitational potential energy of the Tibetan Plateau and the forces driving the Indian Plate. *Geology*, *34*, 321–324.
Gilbert, W. (1986). Origin of life: The RNA world. *Nature*, *319*, 618.
Gilligan, A., Bastow, I. D., & Darbyshire, F. A. (2016). Seismological structure of the 1.8 Ga Trans-Hudson Orogen of North America. *Geochemistry, Geophysics, Geosystems*, *17*, 2421–2433. https://doi.org/doi:10.1002/2016GC006419
Goldstein, S. L., O'Nions, R. K., & Hamilton, P. J. (1984). A Sm-Nd isotopic study of atmospheric dusts and particulates from major river systems. *Earth and Planetary Science Letters*, *70*, 221–236.
Gordon, R. G., & Houseman, G. A. (2015). Deformation of Indian Ocean lithosphere: Evidence for a highly nonlinear rheological law. *Journal of Geophysical Research: Solid Earth*, *120*, 4434–4449. https://doi.org/doi:10.1002/2015JB011993

Grambling, J. A. (1981). Pressures and temperatures in Precambrian metamorphic rocks. *Earth and Planetary Science Letters*, *53*, 63–68.
Grand, S., & Helmberger, D. V. (1984). Upper mantle shear structure of North America. *Geophysical Journal Royal Astronomical Society*, *76*, 399–438.
Grove, T. L., & Parman, S. W. (2004). Thermal evolution of the Earth as recorded by komatiites. *Earth and Planetary Science Letters*, *219*, 173–187.
Gupta, S., Rai, S. S., Prakasam, K. S., Srinagesh, D., Bansal, B. K., Chadha, R. K., et al. (2003). The nature of the crust in southern India: Implications for Precambrian crustal evolution. *Geophysical Research Letters*, *30*(8), 1419. https://doi.org/doi:10.1029/2002GL016770
Hacker, B. R., Kelemen, P. B., & Behn, M. D. (2015). Continental lower crust. *Annual Review of Earth and Planetary Sciences*, *43*, 167–205.
Hanczyc, M. M., Fujikawa, S. M., & Szostak, J. W. (2003). Experimental models of primitive cellular compartments: Encapsulation, growth, and division. *Science*, *302*, 618–622.
Harrison, C. G. A. (1988). Eustasy and epeirogeny of continents on time scales between about 1 and 100 m. y. *Paleoceanography*, *3*, 671–684.
Harrison, C. G. A., Miskell, K. J., Brass, G. W., Saltzman, E. S., & Sloan, J. L. II (1983). Continental hypsography. *Tectonics*, *2*, 357–377.
Hawkesworth, C. J., & Kemp, A. I. S. (2006). Evolution of the continental crust. *Nature*, *443*, 811–817.
Haxby, W. F., & Turcotte, D. L. (1978). On isostatic geoid anomalies. *Journal of Geophysical Research*, *83*, 5473–5478.
Herzberg, C., Condie, K., & Korenaga, J. (2010). Thermal history of the Earth and its petrological expression. *Earth and Planetary Science Letters*, *292*, 79–88.
Herzberg, C., & Rudnick, R. (2012). Formation of cratonic lithosphere: An integrated thermal and petrological model. *Lithos*, *149*, 4–15.
Heubeck, C. E., & Lowe, D. R. (1994). Depositional and tectonic setting of the Archean Moodies Group, Barberton Greenstone Belt, South Africa. *Precambrian Research*, *68*, 257–290.
Hillier, J. K. (2010). Subsidence of 'normal' seafloor: Observations do indicate 'flattening'. *Journal of Geophysical Research*, *115*, B03102. https://doi.org/doi:10.1029/2008JB005994
Hillier, J. K., & Watts, A. B. (2005). The relationship between depth and age in the North Pacific Ocean. *Journal of Geophysical Research*, *110*, B02405. https://doi.org/doi:10.1029/2004JB003406
Hofmann, A. W., Jochum, K. P., Seufert, M., & White, W. M. (1986). Nb and Pb in oceanic basalts: New constraints on mantle evolution. *Earth and Planetary Science Letters*, *79*, 33–45.
Hoggard, M. J., Winterbourne, J., Czarnota, K., & White, N. (2017). Oceanic residual depth measurements, the plate cooling model, and global dynamic topography. *Journal of Geophysical Research: Solid Earth*, *122*, 2328–2372. https://doi.org/doi:10.1002/2016JB013457
Houseman, G. A., & England, P. C. (1986). Finite strain calculations of continental deformation, 1, Methods and general results for convergent zones. *Journal of Geophysical Research*, *91*, 3651–3663.
Hren, M. T., Tice, M. M., & Chamberlain, C. P. (2009). Oxygen and hydrogen isotope evidence for a temperate climate 3.42 billion years ago. *Nature*, *460*, 205.
Hurley, P. M., & Rand, J. R. (1969). Pre-drift continental nuclei. *Science*, *164*, 1229–1242.
Hynes, A. (2001). Freeboard revisited: Continental growth, crustal thickness change and Earth's thermal efficiency. *Earth and Planetary Science Letters*, *185*, 161–172. https://doi.org/doi:10.1016/S0012-821X(00)00368-X
Irvine, G. J., Pearson, D. G., & Carlson, R. W. (2001). Lithospheric mantle evolution of the Kaapvaal Craton: A Re-Os isotope study of peridotite xenoliths from Lesotho kimberlites. *Geophysical Research Letters*, *28*, 2505–2508.
Jaffrés, J. B. D., Shields, G. A., & Wallmann, K. (2007). The oxygen isotope evolution of seawater: A critical review of a long-standing controversy and an improved geologic water cycle model for the past 3.4 billion years. *Earth-Science Reviews*, *83*, 83–122.
James, D. E., Niu, F.-l., & Rokosky, J. (2003). Crustal structure of the Kaapvaal craton and its significance for early crustal evolution. *Lithos*, *71*, 413–429.
Jarrard, R. D. (2003). Subduction fluxes of water, carbon dioxide, chlorine, and potassium. *Geochemistry, Geophysics, Geosystems*, *4*(5), 8905. https://doi.org/doi:10.1029/2002GC000392
Jaupart, C., Labrosse, S., Lucazeau, F., & Mareschal, J.-C. (2015). Temperatures, heat, and energy in the mantle of the Earth (2nd ed.). In G. Schubert (Ed.), *Treatise of Geophysics* (Vol. 7, pp. 223–270). Amsterdam, Netherlands: Elsevier.
Jaupart, C., & Mareschal, J. C. (1999). The thermal structure and thickness of continental roots. *Lithos*, *48*, 93–114.
Jaupart, C., & Mareschal, J.-C. (2011). *Heat Generation and Transport in the Earth* (pp. 464). Cambridge: Cambridge University Press.
Jaupart, C., & Mareschal, J.-C. (2015). Post-orogenic thermal evolution of newborn Archean continents. *Earth and Planetary Science Letters*, *432*, 36–45.
Jaupart, C., Mareschal, J.-C., Bouquerel, H., & Phaneuf, C. (2014). The building and stabilization of an Archean Craton in the Superior Province, Canada, from a heat flow perspective. *Journal of Geophysical Research: Solid Earth*, *119*, 9130–9155. https://doi.org/10.1002/2014JB011018
Jaupart, C., Mareschal, J. C., Guillou-Frottier, L., & Davaille, A. (1998). Heat flow and thickness of the lithosphere in the Canadian Shield. *Journal of Geophysical Research*, *103*, 15,269–15,286.
Johnson, T. E., Brown, M., Gardiner, N. J., Kirkland, C. L., & Smithies, R. H. (2017). Earth's first stable continents did not form by subduction. *Nature*, *543*, 239–242.
Jordan, T. H. (1975). The continental tectosphere. *Reviews of Geophysics and Space Physics*, *13*, 1–12.
Jordan, T. H. (1978). Composition and development of the continental tectosphere. *Nature*, *274*, 544–548.
Jordan, T. H. (1988). Structure and formation of the continental tectosphere. *Journal of Petrology*, 11–37. Special Lithosphere Issue.
Kachingwe, M., Nyblade, A., & Juli, J. (2015). Crustal structure of Precambrian terranes in the southern African subcontinent with implications for secular variation in crustal genesis. *Geophysical Journal International*, *202*, 533–547.
Kamber, B. S. (2010). Archean mafic-ultramafic oceanic landmasses and their effect on ocean-atmosphere chemistry. *Chemical Geology*, *274*, 19–28.
Kamber, B. S. (2015). The evolving nature of terrestrial crust from the Hadean, through the Archaean, into the Proterozoic. *Precambrian Research*, *258*, 48–82.
Kamo, S. L., & Davis, D. W. (1994). Reassessment of Archean crustal development in the Barberton Mountain Land, South Africa, based on U-Pb dating. *Tectonics*, *13*, 167–192.
Kasting, J. F., Howard, M. T., Wallmann, K., Veizer, J., Shields, G., & Jaffrés, J. (2006). Paleoclimates, ocean depth, and the oxygen isotopic composition of seawater. *Earth and Planetary Science Letters*, *252*, 82–93.
Keller, B., & Schoene, B. (2018). Plate tectonics and continental basaltic geochemistry throughout Earth history. *Earth and Planetary Science Letters*, *481*, 290–304.
Kgaswane, E. M., Nyblade, A. A., Juli, J., Dirks, P. H. G. M., Durrheim, R. J., & Pasyanos, M. E. (2009). Shear wave velocity structure of the lower crust in southern Africa: Evidence for compositional heterogeneity within Archaean and Proterozoic terrains. *Journal of Geophysical Research*, *114*, B12304. https://doi.org/doi:10.1029/2008JB006217

Knauth, L. P. (2005). Temperature and salinity history of the Precambrian ocean: Implications for the course of microbial evolution. *Palaeogeography, Palaeoclimatology, Palaeoecology*, *219*, 53–69.
Knauth, L. P., & Lowe, D. R. (2003). High Archean climatic temperature inferred from oxygen isotope geochemistry of cherts in the 3.5 Ga Swaziland Supergroup, South Africa. *Geological Society of America Bulletin*, *115*, 566–580.
Korenaga, J. (2006). Archean geodynamics and the thermal evolution of Earth. In K. Benn, J.-C. Mareschal, & K. Condie (Eds.), *Archean Geodynamics and Environments, Geophysical Monograph Series* (Vol. 164, pp. 7–32). Washington, DC: American Geophysical Union.
Korenaga, J. (2007). Eustasy, supercontinental insulation, and the temporal variability of terrestrial heat flux. *Earth and Planetary Science Letters*, *257*, 350–358.
Korenaga, J. (2008a). Plate tectonics, flood basalts, and the evolution of Earth's oceans. *Terra Nova*, *20*, 419–439.
Korenaga, J. (2008b). Urey ratio and the structure and evolution of Earth's mantle. *Reviews of Geophysics*, *46*, RG2007. https://doi.org/10.1029/2007RG000241
Korenaga, J. (2011). Thermal evolution with a hydrating mantle and the initiation of plate tectonics in the early Earth. *Journal of Geophysical Research*, *116*, B12403. https://doi.org/doi:10.1029/2011JB008410
Korenaga, T., & Korenaga, J. (2008). Subsidence of normal oceanic lithosphere, apparent thermal expansivity, and seafloor flattening. *Earth and Planetary Science Letters*, *268*, 41–51.
Kröner, A. (1985). Evolution of the Archean continental crust. *Annual Review of Earth and Planetary Sciences*, *13*, 49–74.
Labrosse, S., & Jaupart, C. (2007). Thermal evolution of the Earth: Secular changes and fluctuations of plate characteristics. *Earth and Planetary Science Letters*, *260*, 465–481.
Lambart, S., Baker, M. B., & Stolper, E. M. (2016). The role of pyroxenite in basalt genesis: Melt-PX, a melting parameterization for mantle pyroxenites between 0.9 and 5 GPa. *Journal of Geophysical Research: Solid Earth*, *121*, 5708–5735. https://doi.org/10.1002/2015JB012762
Lee, C.-T. A., Caves, J., Jiang, H.-H., Cao, W.-R., Lenardic, A., McKenzie, N. R., et al. (2017). Deep mantle roots and continental emergence: Implications for whole-Earth elemental cycling, long-term climate, and the Cambrian explosion. *International Geology Review*, *60*, 431–448. https://doi.org/10.1080/00206814.2017.1340853
Lee, C.-T. A., & Chin, E. J. (2014). Calculating melting temperatures and pressures of peridotite protoliths: Implications for the origin of cratonic mantle. *Earth and Planetary Science Letters*, *403*, 273–286. https://doi.org/10.1016/j.epsl.2014.06.048
Lowe, D. R. (1980). Archean sedimentation. *Annual Review of the Earth and Planetary Sciences*, *8*, 145–167.
Lowe, D. R. (1983). Restricted shallow-water sedimentation of early Archean stromatolitic and evaporitic strata of the Strelley Pool Chert, Pilbara block, Western Australia. *Precambrian Research*, *19*, 239–283.
Lowe, D. R. (1999). Geologic evolution of the Barberton greenstone belt and vicinity. In D. R. Lowe & G. R. Byerly (Eds.), *Geologic Evolution of the Barberton Greenstone Belt, South Africa* (pp. 287–312). Boulder, CO: Geological Society of America Special Paper 329.
Lowe, D. R., & Byerly, G. R. (1999). Stratigraphy of the west-central part of the Barberton greenstone belt, South Africa. In D. R. Lowe & G. R. Byerly (Eds.), *Geologic Evolution of the Barberton Greenstone Belt, South Africa* (pp. 1–36): Geological Society of America Special Paper 329.
Lowe, D. R., & Fisher Worrell, G. (1999). Sedimentology, mineralogy, and implications of silicified evaporites in the Kromberg Formation, Barberton greenstone belt, South Africa. In D. R. Lowe & G. R. Byerly (Eds.), *Geologic Evolution of the Barberton Greenstone Belt, South Africa* (pp. 167–188). Boulder, CO: Geological Society of America Special Paper 329.
Lowe, D. R., & Tice, M. M. (2004). Geologic evidence for Archaean atmospheric and climatic evolution: Fluctuating levels of CO_2, CH_4 and O_2, with an overriding tectonic control. *Geology*, *32*, 493–496.
Mahan, K. H., Schulte-Pelkum, V., Blackburn, T. J., Bowring, S. A., & Dudas, F. O. (2012). Seismic structure and lithospheric rheology from deep crustal xenoliths, central Montana, USA. *Geochemistry, Geophysics, Geosystems*, *13*, Q10012. https://doi.org/doi:10.1029/2012GC004332
Martin, W., & Russell, M. J. (2007). On the origin of biochemistry at an alkaline hydrothermal vent. *Philosophical Transactions of the Royal Society of London B*, *362*, 1887–1925.
Matsui, T., & Abe, Y. (1986). Evolution of an impact-induced atmosphere and magma ocean on the accreting Earth. *Nature*, *319*, 303–305.
McCulloch, M. T., & Bennett, V. C. (1993). Evolution of the early Earth: Constraints from ^{143}Nd-^{142}Nd isotopic systematics. *Lithos*, *30*, 237–255.
McCulloch, M. T., & Bennett, V. C. (1994). Progressive growth of the Earth's continental crust and depleted mantle: Geochemical constraints. *Geochimica et Cosmochimica Acta*, *58*, 4717–4738.
McGovern, P. J., & Schubert, G. (1989). Thermal evolution of the Earth: Effects of volatile exchange between atmosphere and interior. *Earth and Planetary Science Letters*, *96*, 27–37.
McKenzie, D. P. (1972). Plate tectonics. In E. C. Robertson (Ed.), *The Nature of the Solid Earth* (pp. 323–360). New York: McGraw-Hill.
McKenzie, D., & Bickle, M. J. (1988). The volume and composition of melt generated by extension of the lithosphere. *Journal of Petrology*, *29*, 625–679.
McKenzie, D. P., & Richter, F. M. (1981). Parameterized thermal convection in a layered region and the thermal history of the Earth. *Journal of Geophysical Research*, *86*, 11,667–11,680.
McKenzie, D. P., & Weiss, N. O. (1975). Speculations on the thermal and tectonic history of the Earth. *Geophysics Journal Royal Astronomical Society*, *42*, 131–174.
Mendiguren, J. A. (1971). Focal mechanism of a shock in the middle of the Nazca plate. *Journal of Geophysical Research*, *76*, 3861–3879.
Michaut, C., & Jaupart, C. (2004). Nonequilibrium temperatures and cooling rates in thick continental lithosphere. *Geophysical Research Letters*, *31*, L24602. https://doi.org/10.1029/2004GL021092
Michaut, C., Jaupart, C., & Bell, D. R. (2007). Transient geotherms in Archean continental lithosphere: New constraints on thickness and heat production of the subcontinental lithospheric mantle. *Journal of Geophysical Research*, *112*, B04408. https://doi.org/10.1029/2006JB004464
Michaut, C., Jaupart, C., & Mareschal, J.-C. (2009). Thermal evolution of cratonic roots. *Lithos*, *109*, 47–60.
Molnar, P., & Lyon-Caen, H. (1988). Some simple physical aspects of the support, structure, and evolution of mountain belts, in Processes in continental lithospheric deformation. *Geological Society of America Special Papers*, *218*, 179–207.
Mulkidjanian, A. Y. (2009). Origin of life in the zinc world: I. Photosynthetic, porous edifices built of hydrothermally precipitated zinc sulfide (ZnS) as cradles of life on Earth, Biol. *Direct*, *4*, 26. https://doi.org/10.1186/1745-6150-4-26
Mulkidjanian, A. Y., Bychkov, A. Yu., Dibrova, D. V., Galperin, M. Y., & Koonin, E. V. (2012). Origin of first cells at terrestrial, anoxic geothermal fields. *Proceedings of the National academy of Sciences of the United States of America*, *109*, E821–E830.
Mulkidjanian, A. Y., & Galperin, M. Y. (2009). On the origin of life in the zinc world. II. Validation of the hypothesis on the photosynthesizing zinc sulfide edifices as cradles of life on Earth, Biol. *Direct*, *4*, 27. https://doi.org/10.1186/1745-6150-4-27
Musacchio, G., White, D. J., Asudeh, I., & Thomson, C. J. (2004). Lithospheric structure and composition of the Archean western Superior Province from seismic refraction/wide-angle reflection and gravity modeling. *Journal of Geophysical Research*, *109*, B03304. https://doi.org/doi:10.1029/2003JB002427

Nair, S. K., Gao, S. S., Liu, K. H., & Silver, P. G. (2006). Southern African crustal evolution and composition: Constraints from receiver function studies. *Journal of Geophysical Research*, *111*, B02304. https://doi.org/10.1029/2005JB003802

Nelson, B. K., & DePaolo, D. J. (1985). Rapid production of continental crust 1.7 to 1.9 b.y. ago: Nd isotopic evidence from the basement of the North American mid-continent. *Geological Society of America Bulletin*, *96*, 746–754.

Nguuri, T. K., Gore, J., James, D. E., Webb, S. J., Wright, C., Zengeni, T. G., et al. (2001). Crustal structure beneath southern Africa and its implications for the formation and evolution of the Kaapvaal and Zimbabwe cratons. *Geophysical Research Letters*, *28*, 2501–2504.

Nisbet, E. G., Cheadle, M., Arndt, N., & Bickle, M. J. (1993). Constraining the potential temperature of the Archaean mantle: A review of the evidence from komatiites. *Lithos*, *30*, 291–307. https://doi.org/10.1016/0024-4937(93)90042-B

Niu, F., & James, D. E. (2002). Fine structure of the lowermost crust beneath the Kaapvaal craton and its implications for crustal formation and evolution. *Earth and Planetary Science Letters*, *200*, 121–130.

O'Neill, C. J., Lenardic, A., Griffin, W. L., & O'Reilly, S. Y. (2008). Dynamics of cratons in an evolving mantle. *Lithos*, *102*, 12–24.

Orgel, L. E. (1968). Evolution of the genetic apparatus. *Journal of Molecular Biology*, *88*, 381–393.

Parsons, B. (1982). Causes and consequences of the relation between area and age of the ocean floor. *Journal of Geophysical Research*, *87*, 437–448.

Parsons, B., & Richter, F. M. (1980). A relation between the driving force and geoid anomaly associated with mid-ocean ridges. *Earth and Planetary Science Letters*, *51*, 445–450.

Parsons, B., & Sclater, J. G. (1977). An analysis of the variation of ocean floor bathymetry and heat flow with age. *Journal of Geophysical Research*, *82*, 803–827.

Patel, B. H., Percivalle, C., Ritson, D. J., Duffy, C. D., & Sutherland, J. D. (2015). Common origins of RNA, protein and lipid precursors in a cyanosulfidic protometabolism. *Nature Chemistry*, *7*, 301–307.

Pearson, D. G., Carlson, R. W., Shirey, S. B., Boyd, F. R., & Nixon, P. H. (1995). The stabilisation of Archaean lithospheric mantle: A Re-Os isotope study of peridotite xenoliths from the Kaapvaal craton. *Earth and Planetary Science Letters*, *134*, 341–357.

Pearson, D. G., Snyder, G. A., Shirey, S. B., Taylor, L. A., Carlson, R. W., & Sobolev, N. V. (1995). Archaean Re-Os age for Siberian eclogites and constraints on Archaean tectonics. *Nature*, *374*, 711–713.

Perkins, D. III, & Newton, R. C. (1981). Charnockite geobarometers based on coexisting garnet-pyroxene-plagioclase-quartz. *Nature*, *292*, 144–146.

Poudjom Djomani, Y. H., O'Reilly, S. Y., Griffin, W. L., & Morgan, P. (2001). The density structure of subcontinental lithosphere through time, Earth Planet. *Science Letters*, *184*, 605–621.

Powner, M. W., Gerland, B., & Sutherland, J. D. (2009). Synthesis of activated pyrimidine ribonucleotides in prebiotically plausible conditions. *Nature*, *459*, 239–242.

Pressman, A., Blanco, C., & Chen, I. A. (2015). The RNA World as a model system to study the origin of life. *Current Biology*, *25*, R953–R963.

Pujol, M., Marty, B., Burgess, R., Turner, G., & Philippot, P. (2013). Argon isotopic composition of Archaean atmosphere probes early Earth geodynamics. *Nature*, *498*, 87–90.

Putirka, K. D. (2005). Mantle potential temperatures at Hawaii, Iceland, and the mid-ocean ridge system, as inferred from olivine phenocrysts: Evidence for thermally driven mantle plumes. *Geochemistry, Geophysics, Geosystems*, *6*, Q05L08. https://doi.org/10.1029/2005GC000915

Putirka, K. (2008). Excess temperatures at ocean islands: Implications for mantle layering and convection. *Geology*, *36*, 283–286.

Reading, A. M., & Kennett, B. L. N. (2003). Lithospheric structure of the Pilbara Craton, Capricorn Orogen and northern Yilgarn Craton, Western Australia, from teleseismic receiver functions. *Australian Journal of Earth Sciences*, *50*, 439–445.

Reimink, J. R., Chacko, T., Stern, R. A., & Heaman, L. M. (2014). Earth's earliest evolved crust generated in an Iceland-like setting. *Nature Geoscience*, *7*, 529–533.

Rey, P. F., & Coltice, N. (2008). Neoarchean lithospheric strengthening and the coupling of Earth's geochemical reservoirs. *Geology*, *36*, 635–638.

Rey, P. F., & Houseman, G. (2006). Lithospheric scale gravitational flow: The impact of body forces on orogenic processes from Archaean to Phanerozoic. In S. J. H. Buiter & G. Schreurs (Eds.), *Analogue and Numerical Modelling of Crustal-Scale Processes* (Vol. 253, pp. 153–167). London: Geological Society, London, Special Publications.

Reymer, A., & Schubert, G. (1984). Phanerozoic addition rates to the continental crust and crustal growth. *Tectonics*, *3*, 63–78.

Ricardo, A., & Szostak, J. W. (2009). Origin of life on Earth. *Scientific American*, *301*(3), 54–61.

Richardson, S. H., Gurney, J. J., Erlank, E. J., & Harris, J. W. (1984). Origin of diamonds in old enriched mantle. *Nature*, *310*, 198–202.

Richardson, S. H., Shirey, S. B., Harris, J. W., & Carlson, R. W. (2001). Archean subduction recorded by Re-Os isotopes in eclogitic sulfide inclusions in Kimberley diamonds. *Earth and Planetary Science Letters*, *191*, 257–266.

Richter, F. M. (1984). Regionalized models for the thermal evolution of the Earth. *Earth and Planetary Science Letters*, *68*, 471–484.

Richter, F. M. (1985). Models for the Archean thermal regime. *Earth and Planetary Science Letters*, *73*, 350–360.

Richter, F. M. (1986). Kelvin and the age of the Earth. *Journal of Geology*, *94*, 395–401.

Richter, F. M. (1988). A major change in the thermal state of the Earth at the Archean-Proterozoic boundary: Consequences for the nature and preservation of continental lithosphere. *Journal of Petrology*, *1*, 39–52. Special Lithosphere Issue.

Robert, F., & Chaussidon, M. (2006). A palaeotemperature curve for the Precambrian oceans based on silicon isotopes in cherts. *Nature*, *443*, 969–972.

Rollinson, H. (2017). There were no large volumes of felsic continental crust in the early Earth. *Geosphere*, *13*, 235–246.

Rowan, C. J., & Rowley, D. B. (2017). Preserved history of global mean spreading rate: 83 Ma to present. *Geophysical Journal International*, *208*, 1173–1183.

Rowley, D. B. (2002). Rate of plate creation and destruction: 180 Ma to present. *Geological Society of America Bulletin*, *114*, 927–933.

Rudnick, R. L., & Fountain, D. M. (1995). Nature and composition of the continental crust: A lower crustal perspective. *Reviews of Geophysics*, *33*, 267–309.

Russell, M. J., & Arndt, N. T. (2005). Geodynamic and metabolic cycles in the Hadean. *Biogeosciences*, *2*, 97–111.

Russell, M. J., Daniel, R. M., Hall, A. J., & Sherringham, J. A. (1994). A Hydrothermally precipitated catalytic iron sulphide membrane as a first step toward life. *Journal of Molecular Evolution*, *39*, 231–243.

Russell, M. J., & Hall, A. J. (1997). The emergence of life from iron monosulphide bubbles at a submarine hydrothermal redox and pH front. *Journal of the Geological Society*, *154*, 377–402.

Russell, M. J., Hall, A. J., Cairns-Smith, A. G., & Braterman, P. S. (1988). Submarine hot springs and the origin of life. *Nature*, *336*, 117.

Saikia, U., Das, R., & Rai, S. S. (2017). Possible magmatic underplating beneath the west coast of India and adjoining Dharwar craton: Imprint from Archean crustal evolution to breakup of India and Madagascar. *Earth and Planetary Science Letters*, *462*, 1–14.

Sandiford, M., Coblentz, D. D., & Richardson, R. M. (1995). Ridge torques and continental collision in the Indian-Australian plate. *Geology*, *23*, 653–656.
Sarafian, E., Gaetani, G. A., Hauri, E. H., & Sarafian, A. R. (2017). Experimental constraints on the damp peridotite solidus and oceanic mantle potential temperature. *Science*, *355*, 942–945.
Satkoski, A. M., Lowe, D. R., Beard, B. L., Coleman, M. L., & Johnson, C. M. (2016). A high continental weathering flux into Paleoarchean seawater revealed by strontium isotope analysis of 3.26 Ga barite. *Earth and Planetary Science Letters*, *454*, 28–35.
Schmalholz, S. M., Medvedev, S., Lechmann, S. M., & Podladchikov, Y. (2014). Relationship between tectonic overpressure, deviatoric stress, driving force, isostasy and gravitational potential energy. *Geophysical Journal International*, *197*, 680–696.
Schoene, B., Dudas, F. O. L., Bowring, S. A., & de Wit, M. (2009). Sm-Nd isotopic mapping of lithospheric growth and stabilization in the eastern Kaapvaal craton. *Terra Nova*, *21*, 219–228.
Schubert, G., Stevenson, D., & Cassen, P. (1980). Whole planet cooling and the radiogenic heat source contents of the Earth and Moon. *Journal of Geophysical Research*, *85*, 2531–2538.
Schutt, D. L., & Lesher, C. E. (2006). Effects of melt depletion on the density and seismic velocity of garnet and spinel lherzolite. *Journal of Geophysical Research*, *111*, B05401. https://doi.org/10.1029/2003JB002950
Schutt, D. L., & Lesher, C. E. (2010). Compositional trends among Kaapvaal Craton garnet peridotite xenoliths and their effects on seismic velocity and density. *Earth and Planetary Science Letters*, *300*, 367–373.
Segré, D., Ben-Eli, D., Deamer, D. W., & Lancet, D. (2001). The lipid world. *Origins of Life and Evolution of the Biosphere*, *31*, 119–145.
Sengör, A. M. C (1999). Continental interiors and cratons: Any relation? *Tectonophysics*, *305*, 1–42.
Shapiro, N. M., & Ritzwoller, M. H. (2002). Monte-Carlo inversion for a global shear-velocity model of the crust and upper mantle. *Geophysical Journal International*, *151*, 88–105.
Shirey, S. B., Carlson, R. W., Richardson, S. H., Menzies, A. H., Gurney, J. J., Pearson, D. G., et al. (2001). Archean emplacement of eclogitic components into the lithospheric mantle during formation of the Kaapvaal Craton. *Geophysical Research Letters*, *28*, 2509–2512.
Shirey, S. B., Harris, J. W., Richardson, S. H., Fouch, M. J., James, D. E., Cartigny, P., et al. (2002). Diamond genesis, seismic structure, and evolution of the Kaapvaal-Zimbabwe craton. *Science*, *297*, 1683–1686.
Sim, S. J., Stegman, D. R., & Coltice, N. (2016). Influence of continental growth on mid-ocean ridge depth. *Geochemistry, Geophysics, Geosystems*, *17*, 4425–4437. https://doi.org/10.1002/2016GC006629
Singh, R. N. (2015). Thermal evolution of Indian cratonic lithosphere. *The Journal of Indian Geophysical Union*, *19*, 375–385.
Singh, A., Ravi Kumar, M., Mohanty, D. D., Singh, C., Biswas, R., & Srinagesh, D. (2017). Crustal structure beneath India and Tibet: New constraints from inversion of receiver functions. *Journal of Geophysical Research: Solid Earth*, *122*, 7839–7859. https://doi.org/10.1002/2017JB013946
Sleep, N. H., & Windley, B. F. (1982). Archean plate tectonics: Constraints and inferences. *Journal of Geology*, *90*, 363–379.
Snyder, D. B., Craven, J. A., Pilkington, M., & Hillier, M. J. (2015). The 3-dimensional construction of the Rae craton, central Canada. *Geochemistry, Geophysics, Geosystems*, *16*, 3555–3574. https://doi.org/doi:10.1002/2015GC005957
Sojo, V., Herschy, B., Whicher, A., Camprub, E., & Lane, N. (2016). The origin of life in alkaline hydrothermal vents. *Astrobiology*, *16*, 181–197. https://doi.org/10.1089/ast.2015.1406
Sumner, D. W., & Beukes, N. J. (2004). Sequence stratigraphic development of the Neoarchean Transvaal carbonate platform, Kaapvaal Craton, South Africa. *South African Journal of Geology*, *109*, 11–22.
Sutherland, J. D. (2016). The origin of life-out of the blue. *Angewandte Chemie International Edition*, *55*, 104–121.
Sykes, L. R., & Sbar, M. L. (1973). Intraplate earthquakes, lithospheric stresses and the driving mechanism of plate tectonics. *Nature*, *245*, 298–302.
Sylvester, P. J., Campbell, I. H., & Bowyer, D. A. (1997). Niobium/Uranium evidence for early formation of the continental crust. *Science*, *275*, 521–523.
Szostak, J. W. (2009). Origins of life: Systems chemistry on early Earth. *Nature*, *459*, 171–172.
Szostak, J. W. (2011). An optimal degree of physical and chemical heterogeneity for the origin of life? *Philosophical Transactions of the Royal Society B*, *366*, 2894–2901.
Szostak, J. W. (2012). The eightfold path to non-enzymatic RNA replication. *Journal of Systems Chemistry*, *3*, 2.
Szostak, J. W., Bartel, D. P., & Luisi, P. L. (2001). Synthesizing life. *Nature*, *409*, 387–390.
Tang, M., Chen, K., & Rudnick, R. L. (2016). Archean upper crust transition from mafic to felsic marks the onset of plate tectonics. *Science*, *351*, 372–375.
Tartése, R., Chaussidon, M., Gurenko, A., Delarue, F., & Robert, F. (2017). Warm Archean oceans reconstructed from oxygen isotope composition of early-life remnants. *Geochemical Perspectives Letters*, *3*, 55–65. https://doi.org/10.7185/geochemlet.1706
Taylor, S. R., & McLennan, S. M. (1995). The geochemical evolution of the continental crust. *Reviews of Geophysics*, *33*, 241–265.
Thompson, D., Bastow, I., Helffrich, G., Kendall, J.-M., Wookey, J., Snyder, D., & Eaton, D. (2010). Precambrian crustal evolution: Seismic constraints from the Canadian Shield. *Earth and Planetary Science Letters*, *297*, 655–666. https://doi.org/10.1016/j.epsl.2010.07.021
Toksöz, M. N., Chinnery, M. A., & Anderson, D. L. (1967). Inhomogeneities in the Earth's mantle. *Geophysical Journal Royal Astronomical Society*, *13*, 31–59.
Trefil, J., Morowitz, H. J., & Smith, E. (2009). The origin of life. *American Scientist*, *97*, 206–213.
Trower, E. J., & Lowe, D. R. (2016). Sedimentology of the 3.3 Ga upper Mendon Formation, Barberton Greenstone Belt, South Africa. *Precambrian Research*, *281*, 473–494.
Tseng, T.-L., & Chen, W.-P. (2006). Probing the southern Indian shield with *P*-wave receiver-function profiles. *Bulletin of the Seismological Society of America*, *96*, 328–333.
Turcotte, D. L., & McAdoo, D. C. (1979). Geoid anomalies and the thickness of the lithosphere. *Journal of Geophysical Research*, *84*, 2381–2387.
Turcotte, D. L., & Oxburgh, E. R. (1967). Finite amplitude convective cells and continental drift. *Journal of Fluid Mechanics Research*, *28*, 29–42.
van Thienen, P., Vlaar, N. J., & van den Berg, A. P. (2004). Plate tectonics on the terrestrial planets. *Physics of the Earth and Planetary Interiors*, *142*, 61–74.
Vergnolle, M., Calais, E., & Dong, L. (2007). Dynamics of continental deformation in Asia. *Journal of Geophysical Research*, *112*, B11403. https://doi.org/doi:10.1029/2006JB004807
Vlaar, N. J. (2000). Continental emergence and growth on a cooling Earth. *Tectonophysics*, *322*, 191–202.
Wächtershäuser, G. (1988a). Pyrite formation, the first energy source for life: A hypothesis. *Systematic and Applied Microbiology*, *10*, 207–210.
Wächtershäuser, G. (1988b). Before enzymes and templates: Theory of surface metabolism. *Microbiology Review*, *52*, 452–484.
Wasserburg, G. J., MacDonald, G. J. F., Hoyle, F., & Fowler, W. A. (1964). Relative contributions of uranium, thorium, and potassium to heat production in the Earth. *Science*, *143*, 465–467. https://doi.org/10.1126/science.143.3605.465

Westerlund, K. J., Shirey, S. B., Richardson, S. H., Carlson, R. W., Gurney, J. J., & Harris, J. W. (2006). A subduction wedge origin for Paleoarchean peridotitic diamonds and harzburgites from the Panda kimberlite, Slave craton: Evidence from Re-Os isotope systematics. *Contributions to Mineralogy and Petrology*, *152*, 275–294.

White, R. S., McKenzie, D., & O'Nions, R. K. (1992). Oceanic crustal thickness from seismic measurements and rare earth element inversions. *Journal of Geophysical Research*, *97*, 19,683–19,715.

Wiens, D. A., & Stein, S. (1985). Implications of oceanic intraplate seismicity for plate stresses, driving forces, and rheology. *Tectonophysics*, *116*, 143–162.

Wise, D. U. (1974). Continental margins, freeboard and the volumes of continents and oceans through time. In C. A. Burk & C. L. Drake (Eds.), *The Geology of Continental Margins* (pp. 45–58). New York: Springer.

Youssof, M., Thybo, H., Artemieva, I. M., & Levander, A. (2013). Moho depth and crustal composition in southern Africa. *Tectonophysics*, *609*, 267–287.